energies

MDPI

Article

SPEAR (Solar Pyrolysis Energy Access Reactor): Theoretical Design and Evaluation of a Small-Scale Low-Cost Pyrolysis Unit for Implementation in Rural Communities

Cesare Caputo [1,*] and Ondřej Mašek [2]

[1] Dyson School of Design Engineering, Imperial College London, Imperial College Rd, Kensington, London SW7 1AL, UK
[2] UK Biochar Research Centre, School of GeoSciences, University of Edinburgh, Crew Building, Alexander Crum, Brown Road, Edinburgh EH9 3FF, UK; ondrej.masek@ed.ac.uk
* Correspondence: c.caputo19@imperial.ac.uk

Abstract: Energy access and waste management are two of the most pressing developmental and environmental issues on a global level to help mitigate the accelerating impacts of climate change. They are particularly relevant in Sub–Saharan Africa where electrification rates are significantly below global averages and rural areas are lacking a formal waste management sector. This paper explores the potential of integrating solar energy into a biomass pyrolysis unit as a potentially synergetic solution to both issues. The full design of a slow pyrolysis batch reactor targeted at biochar production, following a strict cost minimization approach, is presented in light of the relevant considerations. SPEAR is powered using a Cassegrain optics parabolic dish system, integrated into the reactor via a manual tracking system and optically optimized with a Monte-Carlo ray tracing methodology. The design approach employed has led to the development an overall cost efficient system, with the potential to achieve optical efficiencies up 72% under a 1.5° tracking error. The outputs of the system are biochar and electricity, to be used for soil amendment and energy access purposes, respectively. There is potential to pyrolyze a number of agricultural waste streams for the region, producing at least 5 kg of biochar per unit per day depending on the feedstock employed. Financial assessment of SPEAR yields a positive Net Present Value (NPV) in nearly all scenarios evaluated and a reasonable competitiveness with small scale solar for electrification objectives. Finally, SPEAR presents important positive social and environmental externalities and should be feasibly implementable in the region in the near term.

Keywords: biochar; concentrated solar power; solar pyrolysis; bioenergy; carbon capture

Citation: Caputo, C.; Mašek, O. SPEAR (Solar Pyrolysis Energy Access Reactor): Theoretical Design and Evaluation of a Small-Scale Low-Cost Pyrolysis Unit for Implementation in Rural Communities. *Energies* **2021**, *14*, 2189. https://doi.org/10.3390/en14082189

Academic Editor: Haftom Weldekidan

Received: 17 March 2021
Accepted: 9 April 2021
Published: 14 April 2021

1. Introduction

1.1. Regional Context and Call for Action

As part of the growing call to address the accelerators of climate change while balancing the demand for growth in developing countries, energy and waste management are two of the most crucial issues to be addressed [1]. It is estimated that 1.1 billion people still have no access to electricity and 2.8 billion still rely on traditional biomass combustion for cooking or heating demand, largely driven by unsustainable forestry practices or consumption [2]. Energy access and electrification have been consistently linked to the Sustainable Development Goals (SDGs) and thus are being increasingly considered together, while helping to mitigate the impact of climate change in developing countries [3].

As a result of particularly vulnerable climate conditions, low development levels and the current lack of appropriate policy frameworks, Sub-Saharan Africa (SSA) is the region expected to be most severely affected by changing climate conditions [4]. In fact, while it is estimated that by 2030 the number of people with no access to electricity will decrease to 674 million, 600 million of those are predicted to be in rural areas of SSA, which currently

still has only a 43% electrification rate [2]. Bioenergy has been identified as one of the most feasible energy access pathways in the region given the vast feedstock abundance; however, its deployment at scale has thus far been largely limited from technical capacity, concerns over competition with food crops and cultural acceptance considerations [5]. Traditional bioenergy systems present significant disadvantages regarding the quality of the provision of energy services relative to the economic and energetic expenditure. They typically exhibit very low efficiencies of 5–20% and are only able to supply low grade heat with limited control methods [6]. The low material energy density implies that a large volume biomass is required to meet daily demands, leading to women and children spending up to 8 h a day on the collection of material in some communities, with negative externalities on deforestation [7,8]. Additionally, 350,000 children and 34,000 adult women are estimated to die every year as a result of health issues associated with indoor and polluting bioenergy consumption [6].

On the other hand, waste management is a more complicated issue to address as a synergetic link with development is less clear to the affected populations. Costly and complex waste processing operations are in direct competition for financing with education, clean water, and economic development projects in low-income countries. Nonetheless, emissions from improper solid waste management and landfilling are responsible for over 5% of total greenhouse gas (GHG) emissions and are predicted to nearly double by 2050. Over 50% of solid waste production in low/middle-income countries comes from green and food sources, with increasing proportions found in more rural areas [9]. In SSA, waste production is predicted to triple by 2050 as there is a lack of appropriate institutional bodies and policy instruments to address it. Currently producing on average 0.46 kg/capita/day, waste generation levels are less than $\frac{1}{4}$ of average North American levels, highlighting the potential for the integration of a more sustainable waste management practices at an early development stage [10]. This is particularly relevant given that Sub-Saharan Africa has significantly higher land per capita than the global average, with by far the lowest energy consumption per capita, and thus the ratio of waste production and bioenergy potential to current demand levels is unique and hints at the role these conversion technologies may play in the coming years on regional sustainable developmental objectives [11].

1.2. Pyrolysis

Pyrolysis is one of the bioenergy conversion pathways which has received the most attention in recent years due to its potential to efficiently convert several forms of biowaste into energy in a sustainable manner. The process is based on the thermochemical degradation of these materials in the absence of oxygen and at elevated temperatures to produce biochar (solids), bio-oil (liquids) and valuable energy content gases [12]. Pyrolysis is typically carried out in lower temperature ranges of 575–1300 K and the final nature of the product is dependent on several parameters, the most important being final pyrolysis temperature, heating rate, particle size and solid residence time, among others. It is normally described as having 3 major phases: moisture evaporation, primary pyrolysis, and secondary pyrolysis. Pre pyrolysis occurs between 373–473 K, consisting of biomass decomposition through internal particle rearrangement, release of free radicals and bound water with some minimal volatilization of the low molecular weight compounds. Following this, primary pyrolysis occurs, which consists of the main decomposition of the solid biomass into the above-mentioned products, normally at a higher rate than the first step. The final stage is secondary pyrolysis, which involves the further decomposition and recombination of primary products, often described as “tar cracking reactions”. These secondary pyrolysis reactions tend to enhance char and gas yields through competing reactions at the expense of condensable vapours, and are thus either enhanced or limited depending on the targeted end-use of the products [13].

The type of pyrolysis and reactor has a very significant effect on pyrolysis product yields; however. ultimately the biomass feedstock composition is the most important factor in determining the final product distribution. This is because the 3 major components of

biomass are cellulose, hemicellulose, and lignin, which all present very different decomposition characteristics arising from fairly independent degradation pathways. Cellulose decomposes over a narrow temperature range of 575–675 K, with negligible char formation associated with it past 750 K and a strong endothermic peak near its peak decomposition temperature. Lignin degradation is much more variable in temperature range and strongly exothermic past 470 K, which have been identified as mechanisms of char formation [14]. Several comprehensive studies have been performed which assess the kinetics and decomposition characteristics of all three components in very fine detail and with varying operational conditions [12–15]. Most recently, a 1–D single particle pyrolysis kinetics scheme for multi-scale simulations showing excellent agreement with experimental results was proposed [16]. The studies and simulations presented in [17,18] represent some alternative state-of-the-art methods and models available for understanding the mechanistic effects driving the process and final product composition.

The application and value of pyrolysis products is still being investigated for its full potential. Biochar is a highly stable and microbial-resistant carbon-rich material, which can be a means of carbon storage for up to thousands of years depending on the way it is produced, although the literature is not in full agreement on the magnitude of this effect [19–22]. The effect on crop productivity is also widely varied, although positive mechanistic effects have been proven experimentally as well as through modeling the biochar impact on direct nutrient provision, pH optimization, improving fertilizer efficiency through soil Cation Exchange Capacity (CEC) enhancement and water holding capacity or drainage dependent on the soil type [20,23]. As part of a recent field survey study 85% of respondents reported yield increases within one year of biochar soil amendment and 10% within 2 years [24]. Biochar can also be used as a direct energy source in some scenarios where other benefits may be more limited, as it presents similar fuel properties to traditional coal, although compromising the sustainability of the process [25].

The produced liquid bio-oil is a relatively low quality fuel, with reduced energy density and flammability relative to comparable fuels [14]. When the scale of the pyrolysis unit allows it, the preferred route for this product is refining and upgrading in order to allow substitution for crude oil in a variety of applications. These additional units have very significant associated cost and engineering design complexity and thus are only economically viable for industrial scale processes [25]. The uses for the pyrolysis gases are more limited as they are non-condensable and contain relatively low energy densities, with higher heating values (HHVs) in the order of 6–10 MJ/kg depending on the feedstock and process employed [26]. The low energy density and resulting limited external applicability means their preferred use is as a means of providing part of the pyrolysis heat requirements through a chamber or external combustion [27]. This allows a higher fraction of the more versatile products to be used in value-added applications, while also minimizing the environmental effects associated with direct pollutant release or incomplete combustion. The ability of these fuels to power the pyrolysis process was recently investigated under a variety of feedstocks and treatment temperatures above 723 K, showing that the lower heating value (LHV) of the gases surpassed the total pyrolysis energy requirements for all feedstocks when estimated as 6% of the original biomass energy content [26]. Flameless oxidation of low quality pyrolysis gases has gotten renewed attention in recent years as it has been proven to release the thermal energy stored within them more cleanly, quietly, efficiently and safely than traditional combustion chambers designs [27–29].

Operating conditions are generally adjusted based on targeted final products, leading to the subclassification of the pyrolysis process into 3 categories: conventional (slow) pyrolysis, fast pyrolysis, and flash pyrolysis. Slow or conventional pyrolysis, the one most relevant to this project given the targeted implementation, has been used for thousands of years and employs a low heating rate and moderate temperatures to favor char formation. The reactors involved are typically less technologically advanced and as a result they tend to suffer from lower yields and relatively increased energy demand from poor heat transfer conditions [30–32]. Regardless of the pyrolysis type, the source of energy used has

a major influence on the overall sustainability and environmental impact of the unit [33]. Autothermal heating methods through the partial combustion of biomass or char, are the most commonly implemented; however, they can reduce product yields significantly and have serious associated environmental consequences. A more detailed review of heat transfer mechanisms implemented for different configurations can be found in [34–36].

1.3. Solar-Powered Pyrolysis

Solar energy has received renewed attention in recent years as a potential sustainable energy source to power the pyrolysis process. Using solar power as the heat source in the reaction allows a higher proportion of the original material to be converted into products when compared to a typical slow pyrolysis process. It also has the potential to significantly reduce pollution levels due to the avoided partial combustions emissions, simplify the heating strategy and allow faster start/up shut down sequences compared to traditional methods [37]. Solar pyrolysis can be broadly classified as either employing direct or indirect heating. In indirect feedstock heating, the material receives heat flux primarily through radiation and conduction from the reactor walls or using a heat transfer fluid (HTF). The use of an HTF, typically molten salt, has been shown to be highly effective in terms of enhanced heat transfer rate to the materials and end-product recovery; however, this necessitates more highly specialized equipment [38]. In the case of indirect feedstock heating and no HTF, performance has been shown to improve drastically when appropriate additional mechanisms to enhance heat transfer rates are implemented [37–40]. In the directly heated concept, the materials are heated directly via concentrated solar radiation through, at minimum, one transparent reactor surface. These kinds of systems, however, are very sensitive to the residence time of reactants in the focal zone for even pyrolysis and window cleaning requirements from tar accumulation. One potential solution may be the combined use of a cavity receiver-type aperture with a high conductivity emitter plate to deliver the heat to the reactor via a bigger radiative surface, previously tested in a hydrogen production solar thermochemical system [40]. This system does not necessitate any sweeping gas or mechanical window cleaning system, as no reactions are happening in the window-topped cavity directly. This configuration, furthermore, increases the total internal reflections (TIR) in the cavity type receiver, leading to a decrease in the delivered flux of only 5% compared to a directly irradiated system [38].

Material compatibility is another important consideration in the design of solar pyrolysis reactors due to the particularly high thermal stresses typically associated with their operation [41]. In direct heating, quartz or borosilicate windows are the preferred material due to their transmissive ability and their ability to withstand temperatures of up to 1500 K and 900 K, respectively, although this can lead to conductive and radiative heat loss in the range of 25–43% [33,37,42]. The insulating and inner materials must also be able to withstand comparable temperatures, large thermal gradients, and high heating rates. Furthermore, the inner materials must be inert to high temperature reducing gases to avoid any unwanted secondary reactions or accidents. In order to achieve the high heat fluxes and temperatures required by the pyrolysis process, flat plate collectors are unsuitable due to the required surface area. Concentrated solar power (CSP) systems, which collect the solar energy and concentrate it onto a single focal point or line, are thus usually the preferred technology, as they have been used for high temperature solar thermochemical processing in several other applications at scale, including water desalination, methane reforming and hydrogen production [41]. The integration of an appropriate CSP system has often been the most important practical barrier to commercial scale solar pyrolysis development, as it can consist of up to 60% of the depreciable capital in a solar thermal processing unit [41].

A solar pyrolysis process using orange peels in a tubular monosilicate glass reactor with a 2 inch diameter mounted on the focal line of a parabolic through concentrator has been more recently proposed and implemented [32]. Using the local direct normal insolation (DNI) of 965 W/m^2, the reactor achieved average temperature of 563 K, peaking

at 738 K during pyrolysis and was able to volatize 77% of the original sample, with 20% char yield by weight [32]. A more complex, fully automated solar concentrator using a Fresnel Lens with 2 degrees of freedom tracking for the pyrolysis of scrap tire rubber at 823 K for 15 min was able to obtain slightly higher efficiencies and increase tar yields. The reactor was tubular and made of quartz; however, this could only accommodate up to 1 g of the sample at the time and thus the design is hardly scalable at the time of writing [43]. The few examples of non-laboratory or pilot scale designs available tend to employ a central receiver system with a mirror or heliostat field to obtain the necessary heat fluxes for the pyrolysis of a bigger amount of feedstock. Recently, one particularly relevant unit was developed for the pyrolysis of jatropha seeds at a capacity of 15 kg/batch [44]. The unit used a Sheffler dish system to achieve a 16:1 concentration ratio onto a circular fixed bed type reactor. No sweeping gas was used for the batches and the char was collected at the end of the operation through an outlet at the bottom. Average reactor temperatures were in the order of 553–623 K, achieving mean conversion rates of 80% and maximum tar and char yields of 20% and 50% by weight respectively, over a 15-day operation. In another recent study, a 6 L Pyrex balloon was irradiated through a heliostat field and a 2 m parabolic concentrator to pyrolyze agricultural and forestry residues under sub-atmospheric (0.52 bar) reactor conditions [45]. In the study by Zhang et al [46], using a vertical axis solar furnace, a beech wood sample was wrapped in graphite foam and thus could only be heated through conduction and convection from produced pyrolysis vapors, employing Argon as a sweeping gas as it is transparent in the applied wavelength region. This study was the first to determine the energy upgrade factor (*EUF*) for solar pyrolysis, a measure of thermochemical conversion efficiency, yielding 1.33 and 1.53 at 875 K and 1300 K, respectively. This compares extremely well to the *EUF* for conventional autothermal pyrolysis (*EUF* = 0.91) or even solar gasification (*EUF* = 1.18) obtained from previous studies with similar feedstocks [31,47]. *EUF* values greater than 1 are indicative of successful and efficient energy storage in the chemical form, which is not normally achieved in conventional autothermal pyrolysis.

1.4. Research Objectives and Structure

The primary aim of this manuscript is the design and feasibility assessment of a solar-powered pyrolysis unit which could be practically implemented in rural communities in SSA, helping to address a gap in the literature on the actual on-field feasibility of this technology to help meet energy access objectives. At the same time, the environmental impact is deemed a crucial factor and thus the reactor should also address waste management, while trying to maximize acceptance with local communities. In this work, we propose a novel design concept based on a Cassegrain optics configuration to address some of the limitations normally associated with small scale low-cost solar pyrolysis, allowing for a simpler, fully manual, and optically efficient operation. The proposed design, accompanied by a theoretical study, is targeted at sustainable development objectives and is different in scale and implementation settings from previous alternatives. The rest of this paper proceeds as follows. In Section 2, the design and assessment methodology implemented is explained, including performance estimation metrics, an example case study and the procedure. Section 3 is concerned with the results from the technical, financial, and environmental evaluation of the system. Section 4 is a discussion on the actual feasibility of the unit, and Section 5 presents conclusions on the additional potential of the system and directions for further research.

2. Materials and Methods

While an attempt was made to design for flexibility as much as possible to allow implementation throughout SSA, there were instances where specific values had to be used to guide system sizing and load analysis. It was therefore determined that in these cases, values for a site estimated to be representative of average conditions in the region would be used. The site chosen is in the Otjozndjupa region of Namibia (−20.465842, 18.4379), a rural

agriculture-based area with very low electrification rates [48,49]. All costs are presented in 2019 USD ($), via the Consumer Price Index (CPI) adjustment for older references [50].

2.1. Potential Feedstocks and Reactor Sizing

The main available potential feedstocks from agricultural and forestry waste streams in SSA are summarized in Table 1 [51,52]. According to thermogravimetric analysis (TGA) from the literature, more than 80% by weight of these feedstocks can be decomposed at temperatures below 823 K with pyrolysis onset temperatures of around 473 K [8,53,54]. This makes them ideal candidates for combination with a solar pyrolysis system due to the relatively lower associated process energy requirements. Furthermore, there is something of a correlation where higher density feedstocks present a lower residue: crop ratio. This combines well with the development of a standardized unit, as similar weight amounts ought to be available from agricultural activity in the different regions considered.

Table 1. Properties relevant to the pyrolysis process for the primary feedstocks considered.

Property	Rice Husks	Sugarcane Bagasse	Corn Straw	Timber Residue	Eucalyptus Residue
Residue: Crop ratio	1:0.67	1:3.3	1:0.77	1:2.3	1:1.8
Pyrolysis Onset Temperature range (K)	473–823	473–723	473–823	498–823	483–903
Recorded Weight Loss (%)	50	65	70	75	80
Bulk Density Dry Basis (kg/m^3)	100	120	130	220	480

Regional wide evaluations estimate that average agricultural waste production rates in the region are in the order of 1.5 kg/person/day [9]. Based on a system to be operated by a small community of 10 people, for compatibility with the lowest feedstock density and a max reactor filling of 80%, to achieve sufficient heat transfer and regional agricultural waste production, the required volume is estimated as:

$$V_{MinimumReactor} = \frac{1.5\frac{kg}{person * day} \times 10\frac{people}{reactor}}{\left(100\frac{kg}{m^3}\right) \times (80\%\, maxfilling)} = 0.1875\ \mathrm{m}^3 \quad (1)$$

The closest match is found with the most common drum size available: the 55-gallon (200 L) cylindrical stainless-steel drum, with new units costing 20–100$ drum [55]. This prefabricated container is deemed a good option, as it presents a very similar volume to the estimated required one, while holding very strong anti-corrosive and thermal properties. A similar approach is followed for sizing various tubing and valve components, using available water pipe dimensions to avoid the need for specialized component manufacture.

2.2. Pyrolysis Heat Transfer Approach and Modeling

A cavity receiver setup was initially designed using the empirical correlations for optimal aperture size through reactor target temperature and a heat flux was previously developed [56–59]. The receiver is implemented as an SiC-coated ceramic emitter plate to provide the radiative heat transfer from the solar unit at the top of the reactor, at approximately three times the rate of steel walls. Batch reactor mixing was not implemented due to the limited feedstock pre-treatment and the desire to maximize simplicity. Two sets of heat pipes were implemented instead. Firstly, an anti-gravity loop heat pipe was designed near the center of the reactor to help spread the radiative energy from the emitter plate into the central and lower sections of the feedstock. This is complemented by vertical capillary heat pipes to carry the energy from the onsite gas combustion into the bottom half of the reactor evenly. The likely feedstock particle density and void ratio for the unit were guiding factors in this selection as they simultaneously reduce the benefits of a mixing system while increasing the need for a good heat transfer mechanism [12]. Details on heat pipe design

can be found in Section 3. Insulation is also essential to complement the heat transfer approach by minimizing the incurred energy losses. Modularity is targeted here to allow for operational optimization at different sites with varying objectives, including changes in material selection. A basic heat transfer model is developed to approximate the heat delivered to the reactor for pyrolysis. The energy limits for pyrolysis gases are estimated via simulation results on some of the lower energy feedstock outlet gas compositions and are checked against the study of self-sustaining pyrolysis in [26]; however, a lower limit of 1.1 MJ/kg is imposed for the calculations here, thus:

$$Qmin_{combustion\ chamber} = 1.1\frac{\mathrm{MJ}}{\mathrm{kg}} \times 0.001864\frac{\mathrm{m}^3}{\mathrm{s}} \times 0.960\frac{\mathrm{kg}}{\mathrm{m}^3} \times 25\%\ \text{efficiency} = 492\mathrm{W} \quad (2)$$

The heat balance of the system is generally estimated as:

$$Q_{solar} = Q_{reactor} + Q_{biomass} + Q_{reactions} + Q_{loss} \quad (3)$$

where $Q_{reactor}$ is composed of the energy to heat both the reactor wall and the cavity receiver/emitter place configuration. $Q_{biomass}$ includes both the energy for moisture evaporation and that to bring the biomass material up to the desired pyrolysis temperature while $Q_{reactions}$ is the heat needed to meet the activation energy for the decomposition of the primary biomass pseudo components. Q_{loss} is instead the energy lost to the environment through combined conduction, radiation and convection phenomena, which is calculated as:

$$Q_{loss} = Q_{optical\ losses} + \sum_{i=0}^{N}[Q^i_{conduction} + Q^i_{convection} + Q^i_{radiation}] \quad (4)$$

where $Q_{optical\ losses}$ is the sum of energy losses from the slope surface errors and non-perfect reflectivity of the low-cost CSP materials and i represents each heat transfer surface, simplified for the purposes of analysis as the receiver aperture plus cavity walls, reactor side walls, insulation, and combustion chamber. Heat losses from other surfaces are thus assumed to be negligible compared to the total system energy flux. The conduction losses are then calculated for each surface as [60]:

$${Q_{conduction\ loss}}^i = (k_i/t_i)A_i(T_i - T_{env}) = h_{cond,i}(T_i - T_{env}) \quad (5)$$

where k represents the thermal conductivity (W/m K), t_i is the conduction medium thickness, A_i is the surface area, $h_{cond,i}$ is the conductive heat transfer coefficient (W/m^2 K) and $(T_i - T_{env})$ is the temperature difference between the reference surface i and the outside environment in K. The radiative losses are estimated from [59]:

$${Q_{radiation\ loss}}^i = \varepsilon_i\,\sigma\left({T_i}^4 - {T_{env}}^4\right)A_i \quad (6)$$

where ε_i is the emissivity of surface i, σ is the Stefan Boltzmann constant (5.67×10^{-8} W/m^2 K^4) and A_i is the radiative surface area. Radiation losses from the bottom wall of the reactor are assumed to be negligible as a very minimal temperature difference will be present there until the combustion chamber starts running, at which point the chamber is expected to experience higher temperatures than the reactor. A linearized version of the radiative losses can also be estimated to simplify the overall heat transfer analysis assuming the temperature difference is not too big, using:

$${Q_{radiation\ loss}}^i = 4\varepsilon_i\,\sigma{T_{mean}}^3(T_i + T_{env})A_i \quad (7)$$

$$T_{mean} = (T_i + T_{env})/2 \quad (8)$$

$$h_{rad} = 4\varepsilon_i\,\sigma{T_{mean}}^3 \quad (9)$$

Convective losses are then estimated as:

$$Q^{i}_{convection\ loss} = h_{convection} A_i (T_i - T_{env})$$

$$h_{convection} = h_{forced} + h_{free} \quad (10)$$

where $h_{convection}$ is the overall convective heat transfer coefficient for the surface, calculated from the sum of natural and forced convective effects at the surface, the magnitude of which is approximated from empirical correlations found in the literature [57,61]. The overall heat loss coefficient U (W/m^{2}K) for the whole system is then approximated for each surface as:

$$U_{loss}{}^{i} = h^{i}_{conduction} + h^{i}_{radiation} + h^{i}_{convection} \quad (11)$$

The heat loss rate for the whole system (W) can then be calculated throughout the process conditions as:

$$Q_{total\ losses} = \sum_{i=0}^{N} U_{loss}{}^{i} A_i (T_i - T_{env}) \quad (12)$$

$$Q_{reactor} = Q_{emitter\ plate\ radiation} + Q_{emitter\ plate\ conduction\ to\ reactor\ side\ walls} + Q_{combustion\ chamber\ conduction\ to\ bottom\ reactor\ wall} \quad (13)$$

$$Q_{biomass} = (Q_{emitter\ plate\ radiation} - Q_{emitter\ plate\ absorbed\ by\ reactor}) + Q_{conduction\ from\ reactor\ walls} + Q_{radiation\ from\ reactor\ walls} + Q_{convection\ pyrolysis\ gases} + Q_{heat\ pipes} - Q_{losses} \quad (14)$$

The effect of the heat pipes on the enhancement of overall heat transfer is included in the heat transfer analysis through an increase in the overall heat transfer coefficient (U) provided to the biomass material, the magnitude of which is estimated above and is dependent on the relative thermal gradient and heat flux at different points of the process [62,63]. Thus, a similar correlation as the one developed for the heat losses can be used, such that:

$$U_{biomass,\ net} = \sum h_{radiation,net} + h_{conduction,net} + h_{convection,net} \quad (15)$$

which is calculated across each surface, yielding the final heat transfer to the biomass as:

$$Q_{biomass,net} = \sum_{i=0}^{N} U_{biomass,\ net}{}^{i} A_i (T_i - T_{env}) \quad (16)$$

All material properties used are the ones given in manufacturer specifications or estimated from the literature when not available. The overall thermal energy efficiency of the system is then defined as:

$$\eta_{thermal} = \frac{Q_{biomass,net}}{Q_{solar\ in}} = \frac{(Q_{solar\ in} - Q_{loss})}{Q_{solar\ in}} \quad (17)$$

All of these calculations are performed using Python Pandas in order to include a basic understanding of how the changes in these parameters throughout the operation affect other conditions and are iteratively computed for temperature steps of 5 K to solve for the reactor conditions at different operational points. The empirical correlations developed by [8,14,22,45] are then used as a means for comparative evaluation of reactor performance in terms of component conversion based on the heat transfer rates obtained.

2.3. Solar Unit

Using average values for Table 1 feedstocks on pyrolysis energy requirements, bulk density and a 2 h operation, the required CSP rating is estimated according to Equation (18) [63].

$$Q_{reactorpyrolis} = \frac{0.9\ \text{MJ}}{\text{kg}} \times \frac{60\ \text{kg}}{\text{batch}} \times \frac{1}{2} = 7.5\ \text{kW} \quad (18)$$

It should be noted that this does not include the contributions of pyrolysis vapors to the heating process or longer acceptable residence times in this reactor, adding an implied safety factor. Several CSP options were considered at this stage; however, the estimated energy requirements, associated collector surface area and tolerance to the tracking mechanism suggested a parabolic dish concentrator with a Cassegrain optic hyperbolic secondary reflector as the most suitable option in this setting. While it presents slightly higher capital cost due to the strongly concave shaped mirrors compared to the other systems, there have been a number of manufacturing techniques proposed in recent years driving significant cost reductions, including aluminum-based coatings instead of glass or a number of segmented-facetted surfaces to achieve the approximate parabolic shape [64]. These systems are also able to achieve the highest optical efficiencies out of the alternative CSPs, with a stronger tolerance for tracking errors, as there is no need for individual mirrors to be operated synchronously in order to minimize shading issues and misalignment with a central receiver tower. This leads to better performance, even in the case of uneven ground levels or manufacturing errors while allowing a simple gravity-based char collection mechanism. The geometrical relationships developed by [63] and the design compromises involved in manufacturing and operation are used to determine initial system sizing, with a basic consideration of structural loads involved. A Monte Carlo ray tracing approach to optical analysis via the TracePro® software (Lambda Research Corporation, Littleton, MA, USA) is then employed to further optimize delivered reactor heat, fully accounting for all material properties and geometries [65–67]. The sun is modeled as a surface source above the solar unit with a standard angular dispersion of $\pm 0.27^{\circ}$ through a Gaussian distribution traced over a set of 1000 rays.

A completely manually operated mechanical tracking system is proposed, with major axis tracking with 2 degrees of freedom, in the azimuth and altitude direction, via a simple guiding wheelbase. The system is designed to be operational for one ~ 2-hour batch per day during peak irradiance to reduce costs and increase compatibility with community lifestyle, while optimizing geometrical alignment between the dish, sun, and receiver. Based on the representative case study location, during these hours the average change in the sun's elevation angle was less than 2° while the difference in azimuth is estimated to be a maximum of 42° [66]. A very basic mechanical telescopic system is implemented to orient the dish towards the appropriate direction for elevation tracking, and minimizing the diversion of electricity produced from valuable development services.

2.4. Financial Feasibility Assessment

Willingness to pay is a metric that can be used to assess the potential value of alternative technologies and it is the maximum price that a customer is willing to pay for a product, related to the perceived marginal benefit [67]. The implementation of the solar pyrolysis unit with thermo-electric (TE) modules and a battery could move these rural communities from Tier 0 to Tier 1 on the energy ladder, which is defined as moving from kerosene to electricity lighting while being able to run it for at least 4 h a day [68]. As such, two 5 W LEDs are to be installed, providing much higher quality lighting than kerosene at a low cost [69]. The leftover electricity per day is calculated by subtracting the daily lighting energy requirements (40 Wh) from the total electricity generated by the TE units (around 110 Wh). The value of the leftover electricity each day is initially estimated from the operational cost of running a diesel generator for the same output, as it is the most prevalent regional alternative. Based on current regional diesel prices, neglecting the cost of transport to the site and assuming standard generator efficiencies, an

estimate of 0.2831$/kWh of consumption is obtained and is used from here [70,71]. The calculated value is in close agreement with the available electricity prices for some of the countries in the region and previous studies [72,73]. The benefit of electrification services provided is thus estimated as the sum of reduced household expenditure on kerosene (7.5$/month [74]) and the value of leftover electricity after lighting of 0.2831$/kWh. The value of biochar potential economic benefits through a community-based carbon credit scheme is then assessed under three scenarios:

- A: No carbon credits;
- B: Carbon credits of 8$/MT as currently existing in South Africa [75];
- C: Community-based system allows participation in EU carbon credit market at current price of 31.67$/MT and based on price forecasts in [76].

The estimates for fertilizer values of biochar are wide-ranging and are necessarily based on a significant number of assumptions on the biochar impact on soil nutrients, pH and ultimately crop productivity [24]. However, for the evaluation of the financial performance of the unit, average values of 12.14$/MT calculated across several crops and soil types will be used [21]. These metrics are in a similar range to those reported by other sources, which are in the order of 7–15$/MT but are heavily dependent on the assumptions used [25,77,78]. Furthermore, it is assumed that all produced biochar can be applied to the farmer's lands, with any extra production being easily sellable in the community at the soil amendment value. The biochar carbon sequestration potential instead uses the data and methodology reported by Mohan et al. [19], which employed slow pyrolysis with similar feedstocks as the ones targeted. This study yields 1.13 g CO_2 eq stored in the soil per g of applied, untreated biochar [19]. The delivered value of biochar is then assessed according to Equation (19). Based on the Stern review on the economics of climate change projects, a discount rate of I = 4% is applied in financial assessment [79]. The Net Present Value (NPV) of the project is then calculated under each scenario according to Equation 20, where CF_t is the net cash flow of the project in year t and i is the discount rate. Maintenance costs are neglected, and a 15-year system lifetime is assumed due to insufficient information to determine otherwise at this stage.

$$Value_{biochar} = \left(12.14\ \frac{\$}{\text{kg}} + \frac{1.13\ \text{kg}\ CO_2}{\text{kg Biochar}} \times \text{Carbon price}\left(\frac{\$}{\text{kg}}\right)\right) * \text{Biochar yield(kg)} \quad (19)$$

$$NPV = \sum_{t=0}^{N} \frac{CF_t}{(1+i)^t} \quad (20)$$

2.5. Provision of Electrification Services

In order to capture the full value of the unit and enhance the contribution to sustainable development in the region, the inclusion of a thermoelectric (TE) unit and battery is considered. This choice is made to avoid the need for expensive upgrading equipment of low-quality pyrolysis products while minimizing associated system emissions. The value of electricity estimated in the region means the marginal NPV of purchasing any TE units is negative; however, the consideration to provide a means of electricity generation is essential and primarily due to the desire to enhance social development in these communities. The heat transfer model from Section 2.2 is used to estimate the temperature profile around the reactor and combustion chamber. Implementing the units on the reactor wall is deemed unpractical as it would lead to significant heat losses, complexity of installation and reduction in useful life from the reactor environment. Furthermore, given that high-temperature TE units are over ten times the price of those designed to operate with max hot side temperatures of 673 K, suitable areas to implement lower cost units were primarily investigated as discussed in Section 3.3 [80].

3. Results

3.1. Reactor Design

The section view and dimensions of the SPEAR reactor design is given in Figures 1 and 2, respectively.

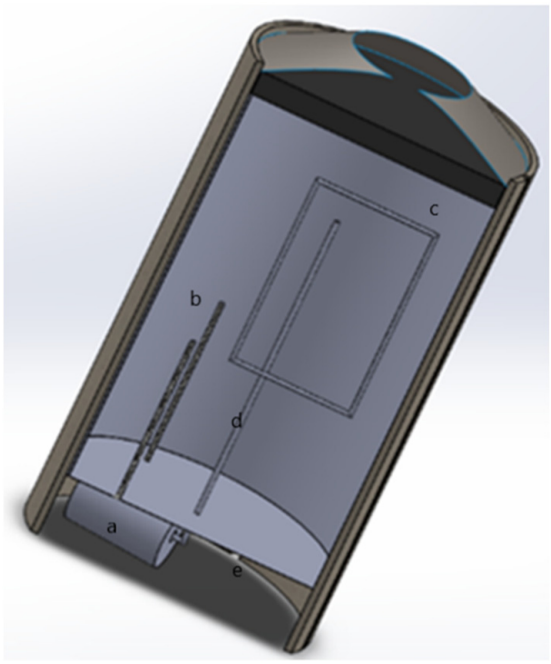

Figure 1. Section view of reactor including: (**a**) flameless oxidation chamber; (**b**) capillary wick heat pipes; (**c**) anti-gravity loop heat pipes; (**d**) gas suction pipe; (**e**) secondary combustion chamber with air inlet holes.

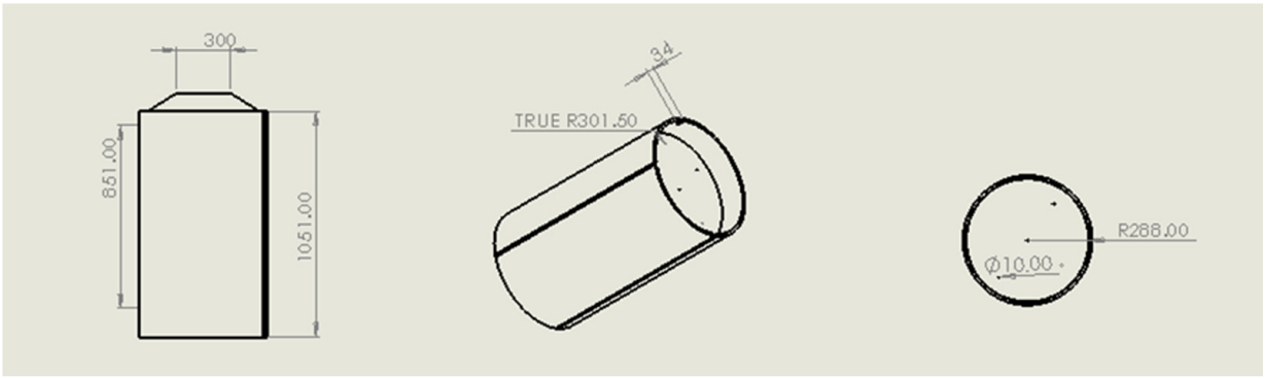

Figure 2. SPEAR system dimensions: reactor and insulation side view (**left**); bottom isometric view showing air inlet holes into chamber (**center**); bottom view showing reactor diameter and capillary heat pipe placement (**right**). All dimensions in mm.

While the primary structure of the steel drum was kept the same, a few adjustments were made in order to allow compatibility with the pyrolysis process. Firstly, the lid at the top is removed completely in order to allow combination with the cavity receiver-emitter plate system shown in Figure 3.

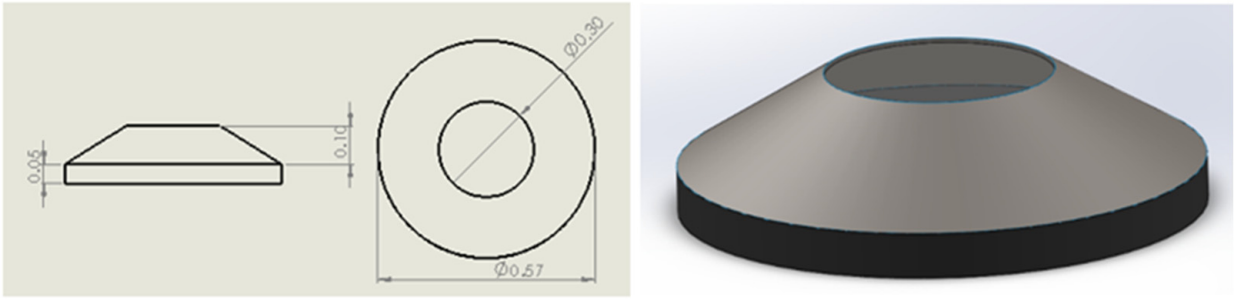

Figure 3. Cavity-receiver and emitter plate configuration design: side view (**left**); top view (**center**) and isometric view (**right**).

The emitter plate's diameter is slightly lower than the inside drum diameter, allowing it to be removed when inputting the feedstock and then be clamped down with air-tight and thermal resistant seals for operation. The proposed system consists of a primary "mini combustion chamber", shown inside of the slightly larger cement insulated chamber, which allows the easy inclusion of heat pipes in the unit without the need to modify the design of the FLOX ™ (WS, Renningen, Germany) system directly. The use of a secondary chamber also allows further cooling of the flue gas before being collected and released by a valve connected exhaust the top of the secondary concrete chamber. The valve is initially closed during the reactor heat-up phase of the unit to ensure appropriate flow patterns and mixing ratios are achieved but is later opened once the gas production is sufficient to avoid unwanted backdraft in the chamber. The materials chosen for the seals and gaskets at the various openings in the reactor are high temperature resistant silicone combined with aluminum gaskets installed through a push on the gasket joint method to obtain the necessary atmospheric conditions inside the reactor [81]. The use of an inert gas is deemed unnecessary due to the batch nature and atmospheric pressure of the reactor as well as the targeting of biochar production, lowering capital and operational costs for the unit. The char is collected at the end of operation through a retrofitted cast iron pipe with a ball valve at the base of the reactor. The char collection pipe empties directly into a plastic bucket once the residue has cooled down sufficiently to allow simple and easy collection. The pyrolysis vapors are collected through a 32 mm tube running through the center of the reactor which is directly coupled to the combustion chamber as to further simplify the design and operation based on the Venturi effect.

A comprehensive analysis of previous designs and material availability yielded cement mixed with combusted charcoal (or ash) as the optimal insulator. The resulting insulation system presents a thickness of 25 mm, with a 1:2:4 Cement: Bottom Ash: Stone Aggregate Ratio, yielding a U value of 2.39 W/m^2K [82]. In addition to providing a low cost and environmentally friendly option for thermal performance, the design includes an overextension at the bottom of the insulating layer on 4 different symmetrical locations in order to fix it to the ground and increase structural reliability. A respective set of 4 symmetrical square openings are left around the insulation in the combustion chamber section to allow creation of the necessary turbulent flow regime for flameless oxidation. The ease of local manufacturing and low cost allows the implementation of a modular design for the insulating layer, increasing the simplicity of replacements and reducing degradation issues.

3.2. Heat Pipes

Table 2 below presents the final parameters defining heat pipe design for SPEAR.

Table 2. Heat pipe final parameters for both configurations.

Parameter	Heat Pipe A	Heat Pipe B
Heat Pipe Type	Anti–gravity loop	Vertical Capillary Wick
Number of Pipes	1	2
Evaporator Energy Source	Radiative, Emitter plate	Convective, Gas combustion
Working Fluid	Water	Dowtherm A™
Fill Level (%)	25	40
Optimal Temperature Operating Range (K)	303–560	423–668
Density at 25 °C (kg/m^3)	997	1056
Pipe Diameter(mm)	8	10
Pipe Material	Stainless Steel	Stainless Steel
Pipe Total Length	400 mm (height) × 250 mm (width)	350 mm
Wick Material	Sintered Copper Powder	Nickel Powder
Wick Permeability	54%	64%
Evaporator Wick Size	75 µm	NA
Liquid Line Wick Size	100 µm	15 µm
Average Thermal Resistance	0.15° K/W	0.1171° K/W
Maximum Deliverable Heat	575 W	375 W per pipe

A more in depth overview of the relevant parameters to heat pipe design and material construction is given in [83]. The anti-gravity operation of heat pipe A is based on previously published work which showed excellent experimental performance, with efficiency values extrapolated based on reactor-specific working conditions [84]. Water is selected as the working fluid for heat pipe A as while it is not as effective in the latter stages of the pyrolysis process due to the elevated process temperatures, it is the most appropriate way to achieve good heat transfer at low cost in order to accelerate the release of the volatiles whose combustion is used as the energy source in heat pipe B to further enhance heat transfer. While water mixed with acetone yielded better properties in terms of heat carrying ability, it was determined that water alone would be preferable to avoid the need to integrate a chemical waste management system. The height in the reactor of heat pipe B was limited to 400 mm in order to facilitate the design and operation of the pipe through ensuring an adequate temperature differential between the evaporator and condenser sections as well as target heat spreading to the bottom part of the reactor, which is less exposed to solar radiation. Dowtherm A™ is selected as the working fluid in heat pipe B as it is easy to obtain due to mass production from the company and exhibits physical and chemical properties which suit the targeted temperature operation range perfectly. Furthermore, the Dowtherm company has a credit program for returning old fluid once useful lifetime limits are approached and operates globally. The selected fluid is also very safe in terms of flammability, presents limited corrosivity and is completely biodegradable and is thus much more environmentally friendly than some of the other alternatives, such as mercury, cadmium, or ammonia [85]. The wick here is not sintered as capillary force limitations are less restricting and allow lower-cost manufacturing to be implemented while still guaranteeing a reliable performance. The sonic, capillary, viscous, and entrainment limits for both designs have been checked against reference curves provided in [86] and are based on the predicted "worst case" operating conditions for the pipes; the system parameters will remain below 15% of the limits. The thermal resistance is calculated from chosen materials, wick type and porosity while the estimated max heat flux carrying capacity is based on the latent and sensible heats of the fluids in the range of operating conditions predicted. The heat pipe set A is placed on the opposite side of

the combustion chamber exhaust outlet where heat transfer from the chamber will be higher based on the provided temperature profiles for the flow regime and thus in order to attempt to balance the system heat transfer further.

3.3. Solar Unit

The resulting designed CSP unit consists of a primary concentrator made of Glass PU sandwich panels, a secondary concentrator made of Sandwich aluminum facets, a quartz cavity receiver, and a mild steel secondary support structure, with optical properties obtained from the literature [64,87,88]. The final configuration for the CSP system is summarized in Table 3, while visual representation of the concentration ability of one of these designs is shown in Figure 4.

Table 3. Selected Cassegrain Optics Configuration.

F_1 (m)	D_2 (m)	F_2 (m)	H_1 (m)	H_2 (m)	SD (m)	A (°)	$\eta_{optideal}$ %	$\eta_{opt\ 1.5°TE}$ %	Q_{cavity} *Ideal* (kW)
2	0.5	0.2857	0.3828	0.0547	1.77	47.26	85	72	6.5

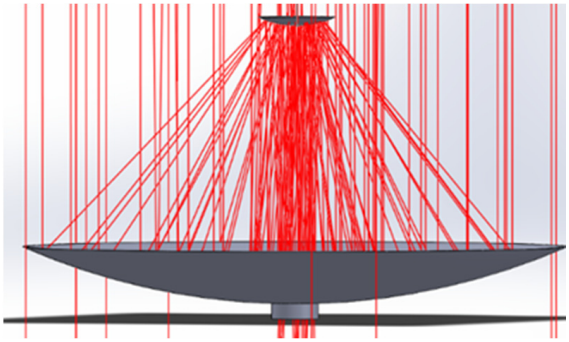

Figure 4. Output of TracePro Optical efficiency optimization.

The primary concentrator is composed of 2 separate pieces which are clamped together at the beginning of the batch process after the feedstock has been loaded. This allows them to be separated at the end of the process for easier maintenance of the reactor and simplifies the collection of any leftover solid residue at the bottom of the reactor. In order to provide an initial safety estimate for the unit, a load analysis was also performed in SolidWorks based on the weight of each part, wind loads, rotational torque and thermal stresses, as shown in Figure 5. The main output was that no stresses were significant enough on the unit to be a cause of concern, although assumptions were quite general at this stage. The char collection pipe is shown in blue for visual clarity.

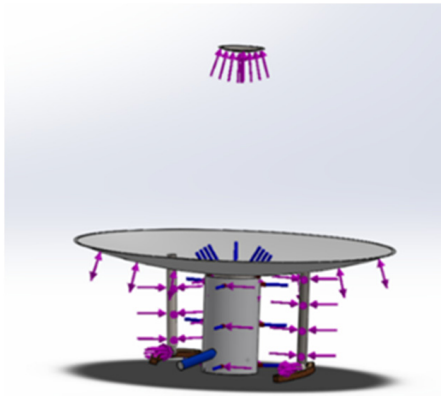

Figure 5. 3D render of CSP system and pyrolysis reactor with load simulation, excluding secondary support poles for clarity.

3.4. Biochar Yield and Provision of Electrification Services

The CSP design presented in Table 3 and the heat transfer model developed in Section 2.2 can be combined with the empirical correlations from the literature to preliminarily estimate reactor performance in terms of component conversion [8,14,22,45]. The results summarized in Table 4 suggest that a minimum volatile conversion rate of 65% and a char yield of 20% by weight should be achievable for all targeted feedstocks. Simulations of reactor heat transfer suggest thermal efficiencies above 70% throughout the expected operational range, with achievable temperatures of up to 750 K. Only slow pyrolysis, therefore, is deemed achievable using SPEAR, also due to the limited temperature control loops integrated at this scale. Using the manufacturer supplied temperature profile distributions and simulation results for gas outlet temperature, lower cost unit operating conditions should be reliably met in the area immediately adjacent to the FLOX™ chamber intake point as well as near the air inlet holes for the insulation layer. Based on the individual unit's dimension and estimated temperature profile, it was deemed possible to implement up to 41 of these low-cost units, yielding a maximum feasible capacity of up to 240 W electricity across the feedstocks evaluated. SPEAR design implements 5 of these units in series with an average thermal-to-electrical conversion efficiency of 6% based on the predicted conditions. Combination with a 220 Wh battery is thus estimated as sufficient to satisfy current local demand for electrification services, with further expansion potential to expand as needed [89,90]. Higher cost and temperature-resistant TE units or a more detailed heat transfer analysis could yield more precise conclusions on the most efficient ways to increase electricity generation capacity and capture a higher proportion of thermal energy release if needed.

Table 4. Estimated yields of different feedstocks using literature correlations. M_{max} denotes the maximum weight of the feedstock that can be loaded for one batch into the reactor based on bulk density and $Q_{minimum}$ (kW) the solar flux necessary to achieve a char yield of 20% for the different feedstocks, not accounting for additional heat losses, using kinetic model from [91].

Parameter	Rice Husk	Sugarcane Bagasse	Corn Straw	Pine Residue	Eucalyptus Residue
M_{max} (kg)	17.7	21.3	23.0	39.1	85.13
$Q_{minimum}$ (kW)	1.147	1.33	1.43	2.55	5.59
Char Yield After 2 h (kg)	6.03	6.17	5.31	12.09	15.32
Char Yield (% wt)	34	29	23	30	18

3.5. Financial Feasibility Evaluation

The full breakdown of the cost of all of the components is given in Table A1 in Appendix A, including references for every single material or parameter used, yielding a total capital cost of 1,237$. This is an order of magnitude lower than any other designs whose cost data were presented in the literature, helping to achieve positive NPVs in all scenarios as shown in Table 5. Furthermore, it is only slightly higher than previously reported costs for actual implementation of a non-solar drum kiln, adding validation to the cost estimation methods used [92]. Major components in the capital costs were reflecting surfaces for the concentrators (32%), battery and TE units (24.2%), heat pipes (16.8%), and the combustion chamber (7.7%).

Table 5. NPV results for the three scenarios presented with five different feedstocks.

Scenario	Rice Husk	Sugarcane Bagasse	Corn Straw	Pine Residue	Eucalyptus Residue
A: NPV (2019$)	223.63	273.07	298.72	526.01	1181.35
B: NPV (2019$)	484.85	586.67	753.67	1295.85	2860.85
C: NPV (2019$)	1258.11	1514.44	1643.69	2802.0	6147.4

4. Discussion

4.1. Biomass Feedstock

Based on this initial analysis, the reactor should be able to achieve the near complete pyrolysis of all potential feedstocks presented, albeit the time estimated for some exceeds the 2-h residence time targeted. Higher density feedstocks seem to produce better financial performance, although a more detailed heat transfer model would help clarify this. The targeted char production means there is more room for error for in the pyrolysis process, as there is no reason to inhibit secondary tar cracking reactions given it is not collected. The reactor could therefore be allowed to run for longer than 2 h if needed, as even if no more manual tracking adjustments are made to minimize the impact on the farmers routine, the CSP system will still be delivering flux to the reactor (albeit at much lower optical efficiencies), which, combined with the exothermic peaks associated with the later stages of component decomposition, is expected to lead to acceptable overall conversion rates. Lower density agricultural residues are pyrolyzed more easily; however, they are limited by the same property on their max char production potential and net product energy content as they present lower biomass HHV to begin with than woody residues. Nonetheless, agricultural residues are expected to be much more easily available based on the implementation in rural farmer communities and the crop–residue ratios presented in Section 2, thus the reactor compatibility with them is more important to its sustainable and practical implementation. There is potential to further investigate-cost efficient mechanisms for the unit to allow more granular temperature control over the process, to achieve higher operating heat fluxes, and to optimize conditions based on feedstock composition. These would likely involve improvements in CSP tracking efficiency to achieve temperature profiles more compatible with complete pyrolysis of around 900 K and a more detailed understanding of internal kinetics.

4.2. Design Considerations and Potential Improvements

The overall impact on a farmer's ability to perform usual labor should be minimal as other than CSP tracking, the only operations required as of now are the loading of the feedstock at first and the collection of the char at the end of the process. It is also expected that these units would be constructed very close to the farmers home or land in order to maximize simplicity of feedstock collection and unit operation, increasing the likelihood of acceptance by the surrounding communities. Based on the feedstock availability and the local output demand, it could also be deemed appropriate to use the reactor for more than 1 batch per day. Depending on the extent of this decision, the lifetime of the unit may be significantly reduced as low-cost materials were the preferred choice for many components. Nonetheless, all selected materials present acceptable resistance to corrosivity and thermal shocks expected from operation and thus with minimal maintenance should be able to allow long-term operation. Tar accumulation on these surfaces may also become problematic depending on the temperature gradient and gas content present at the end of the batch process. The ability to remove the lid of the reactor should optimize the simplicity of cleaning or replacing this pipe if needed. A full understanding of thermal energy release could be combined with additional heat demand for other processes or services in the community and further enhance the economic viability of the unit. In terms of the efficiency of the pyrolysis process, minimizing the feedstock particle size and the drying rates are regarded as highly advantageous in terms of heat transfer rate and energy requirement performance [13,93]. However, achieving the required pretreatment for the majority of the feedstocks considered is likely to be very time-consuming and the improvements in yield are more limited in a simpler system with less control loops such as the one implemented. The use of a mechanical clock-based system for the azimuth wheel tracking base was considered at first; however, the wide range of latitudes proposed means the relative sun speed in the sky is not constant across all sites and thus no generalized design can be made. A mechanical clock-based system would still be highly beneficial and could certainly be included in later iterations of the design as it would serve the

dual purpose of reducing the impact on an operator's routine while also minimizing and standardizing tracking error encountered. Such a system, however, does increase both the cost and manufacturing complexity of the unit compared to the current proposal. The use of a secondary concentrator or transparent homogenizer could also further improve performance under angular dispersion.

4.3. Financial Feasibility

The financial assessment presented in Section 3 shows overall very promising results for the unit. The cost for all system components were directly obtained from a source or manufacturer and are thus expected to be representative of real unit cost. The NPV was positive in all scenarios assessed and the internal rate of return was significantly higher than the discount rate applied to the project. This is essential to practical feasibility of the project as the source of financing for these units is still undetermined and some sort of incentive scheme would likely have to be implemented to allow rural farmer communities to purchase the system. Even though the current cost is extremely low relative to other pyrolysis systems, it is still more than the average annual income reported in the region [94]. One example program in this regard is the one implemented by SolarAid, which saw an increase in uptake by lower income families of up to 35% in some areas through a cost recovery tariff for investment [95].

The factors which are most essential to the economic viability of the system are the biochar yield per batch, value of biochar on soil amendment, carbon credit valuation and the calculated value of electricity access. A basic sensitivity analysis was run including a variation of all 4 of them through 3 scenarios, but using only data for Rice Husks as they had the lowest performance across all financial metrics assessed. The biochar value on soil amendment is a particularly important issue given the vastly different values reported in the literature. As expected, if a non-positive soil amendment value is used for the produced biochar and in the absence of carbon credits, the project NPV remains negative under all biochar production rates. Utilizing the biochar as a fuel source could, in these extreme cases, provide an alternative pathway to economic feasibility. Biochar yields greater than about 5 kg/batch for rice husks are calculated as necessary to achieve a positive NPV. The system financial feasibility is much more sensitive to the price of carbon than that of electricity, showing the importance of developing a carbon market in the region to incentivize emissions reductions programs. The minimal effect of electricity price was expected given under the current design scale the generation capacity is quite low and thus the system is limited as to how much it can internalize increases in the perceived value of electricity. Overall, however, the system maintains a positive NPV across almost all sensitivity scenarios except for extremely low char yields or negative impact on soil productivity. In future iterations of the project, it would be interesting to explore the break-even size for which the inclusion of a condensation and upgradation unit for the pyrolysis vapors leads to a net increase in NPV of the system, particularly as it can substitute household expenditures on diesel or other lower quality fuels, as well as provide a sustainable source for the production of high value chemicals [11].

4.4. Environmental and Social Impact

The environmental and social impacts associated with the project are numerous and overall, the system is expected to perform extremely well in both metrics. The positive environmental impact of a pyrolysis system comes from the combined effect of a reduction in kerosene used for lighting, diesel used for electricity generation and an increase in highly stable carbon stored in the soil from biochar application, reducing the need for chemical fertilizers [24,96]. The use of solar power as the energy source further increases the sustainability of the system by decreasing emissions associated with autothermal combustion. The minimization of organic matter left to decompose in the open or burned on cropland, which has a substantial amount of GHG emissions associated with it also presents very important environmental benefits for the region [97]. This is particularly

relevant considering the lack of a proper waste management plan in most of the region, which leads to a substantial number of landfills and improperly discarded waste. A large portion of this waste is also made up of plastic, negatively affecting soil properties and contaminating the already limited water supply, which has been successfully pyrolyzed in combination with agricultural residues in the past [96]. Furthermore, plastic presents lower activation energies than those reported for lignocellulosic components in most cases, and thus could allow a larger amount of feedstock to be processed with the existing CSP unit. Finally, the use of biochar for contaminated soils or water remediation presents significant potential for future use [24,78].

The social impact and performance of the unit is highly correlated to the movement of these affected communities from Tier 0 to Tier 1 on the energy access ladder and potentially further. On the one hand, the electrification to the region allows an increases in productive work hours at home as lighting can be more cheaply and reliably obtained to complete any necessary tasks. In addition to businesses, the main beneficiaries of electrification services in rural communities in SSA are children, 54% of which are reported as being able to do on average 0.8 h more of homework at night thanks to the addition of lighting [98]. The same survey also yielded that electrification can be a powerful tool for women to develop professionally in these low-income areas, with 41% reporting being able to do extra paid hours of work during the day and increases in family income. Social acceptance of the system, although they are in very traditional communities, is also expected to be quite strong. The impact on the farmer's daily routines is kept extremely limited on purpose, with a proposed implementation on their farmland to allow compatible integration into their activities. The feedstock residues would only be burned or left in the open, otherwise they are not competing with traditional biomass use as would be the case for pure wood materials, for example. Nonetheless, educational awareness on the potential impacts on health, safety and crop productivity of the unit will be essential to ensure widespread implementation within the targeted communities [53].

4.5. Comparison to Alternatives

In order to fully understand the value of SPEAR and its implementation, it is imperative to understand how it performs relative to the current state-of-the art alternatives. The local context is particularly important here, as in the targeted communities in SSA, for example, demand for electrification of services remains very low as of now while reliance on agricultural activities remains high. As such, the design presented is particularly focused on electricity as a vector for sustainable development, rather than on optimising absolute technical performance. When directly evaluating the provision of electrification services, solar home systems (SHS) are the most competitive and prevalent alternatives. A large-scale study of solar PV installations in Africa found that for most systems, capital costs tend to average between 4$/W and 11$/W for sub 1kW installations [95]. In SPEAR, installation cost of TE units averaged 3.5$/W of installed capacity [99]. This compares favorably to the cost of solar PV if no costs for the reactor are included in this consideration, as they bring added value through other mechanisms such as soil amendment, carbon storage and waste management. In the case where these other mechanisms do not apply, the reactor costs may be included with the TE unit capital. Given average annual solar capacity factors in the region of about 15%, a solar unit of 32 W could roughly provide the same daily output power as the TE units. Assuming that installation costs are in the middle of the range at 7.5$/W, a solar unit would thus provide a lower overall initial investment cost per electricity generation capacity compared to SPEAR, given no further added benefits.

The relative financial performance of a PV system compared to SPEAR is preliminarily evaluated to determine the point at which one system becomes advantageous over the other, using the lowest performing feedstock (rice husks). The added value for the PV system electricity is estimated as explained in Section 2. This analysis finds that in the absence of a carbon credit market or soil amendment value for biochar, a SHS system

significantly outperforms SPEAR in economic terms when including reactor costs. In the case that no soil amendment value is present, but a carbon market exists, SPEAR outperforms SHS on NPV delivered for a carbon price past around 38$/MT. In the case of no carbon market, the soil amendment value would have to exceed around 43$/MT, which is more than three times the value used in our analysis and is likely unrealistic. In the presence of both a strong carbon market and soil amendment value (i.e., Scenario C), the installed cost of solar PV would need to be less than about 3.2$/W for it to compete with SPEAR, which, while feasible, is unlikely to be achieved in such small-scale installations unless there is some method of bulk procurement. Increases in the value of electricity, within reasonable bounds, are also not enough on their own for SHS to outperform SPEAR given that most electricity produced is used for lighting. SPEAR also has the advantage that once the reactor is built, scaling up electricity production to match demand evolution presents a much lower marginal cost than SHS.

In terms of energy access, cook stoves and solar thermal are two additional alternatives with some overlapping objectives. Emissions from traditional cookstoves can raise significant concerns related to indoor air pollution and health impacts in these communities [100]. Improved designs present increased efficiency, leading to reduced fuel consumption and pollution, via features such improved flow control and thermal insulation [101]. Cook stoves are also able to provide a means of electricity generation if combined with a TE module as was previously shown, although there are significant limitations to how many can be safely and efficiently installed given the reduced contact area [102]. Furthermore, as part of this study, the authors found that TE units can outperform solar PV in a small scale on a per W basis, further validating our findings from above. Pyrolytic cookstoves, which target biochar as a byproduct of stove operation to be used for soil amendment purposes, are another promising alternative with many parallel objectives to the one proposed in this paper, able to achieve significant reductions in energy required for cooking compared to traditional stoves [103]. The actual biochar production potential in the designs surveyed is, however, very limited as optimal parameters for cooking rather than pyrolysis are prioritized. Furthermore, the implementations found in the literature tend to release significantly more emissions and reduce the carbon capture potential than through a pyrolysis-targeted reactor, with limited conversion efficiencies [101]. In solar thermal applications, irradiation is normally absorbed by a collector and then transferred to a working fluid to provide hot water, heating, storage or to run an engine to generate electricity [104]. When evaluating the technology directly for electricity generation, solar thermal likely would outperform SPEAR as it operates with net solar to electrical conversion efficiencies of 15–35%, as well as large storage capacity. The costs for solar thermal systems, however, tend to be significantly higher than the ones estimated here and tolerances to tracking errors much smaller, thus a more complex and costly design would likely be required [105]. As a result, per kWh electricity costs tend to be higher than with solar PV when storage requirements are smaller than 3 h/day, such as in the targeted implementation, with much higher maintenance needs [106].

Therefore, cookstoves are limited compared to SPEAR as they are not able to scale up TE production as easily for increased electricity demand and/or present very low biochar conversion rates, preventing them from internalizing soil amendment values and carbon market potential. They are, however, likely to provide a simpler and cheaper solution to address improved energy access for cooking in this context. Similarly, solar thermal is limited by complexity and cost while not addressing waste management issues, soil amendment or carbon sequestration. If a stronger demand for heating or storage were present, nonetheless, solar thermal remains a promising alternative. Rather, SPEAR seems to outperform all reasonable alternatives when evaluating the objectives, and it was targeted for more holistically. No other system has been found, to the authors knowledge, that provides electrification services to rural communities in SAA while helping to address land degradation, agricultural productivity, and waste management with a minimal impact on local communities. We thus make the argument that while there are several technologies

better-suited to address individual facets of the problem, none can provide as complete a sustainable development system solution as the one presented here.

4.6. Potential for Scale Up

The advantages of a continuous pyrolysis process in terms of ability to control outputs and optimize yields remain and should be investigated further in future iterations of the project. A potential implementation pathway would be through a community-based pyrolysis unit, with operators rotating and feedstock collection among the various community members. This kind of unit could allow for more electricity and energy byproduct production, which as rural communities continue moving up the energy ladder will become increasingly important. However, such a large-scale system would necessarily have to be designed for more specific kinds of feedstocks and operating conditions in order to internalize the benefits of a more complex control unit. Therefore, while it may be able to provide a better solution for energy access and development in the region, the implementation of a large number of more flexible smaller units such as this one is likely to present better performance in terms of local acceptance, waste management issues and deployment rate. The ability for each family to own a unit directly would increase the value they perceive of it and would likely lead to more overall use as less capital risks and financing limitations are present for such a system [3].

A web–based mobile application could also be developed to optimize site-specific system control if many these units were deployed. The system control application, which could be named "USolPyr", would come complimentary with SPEAR and would be able to provide real-time feedback on average environmental conditions based on the customer's location, warning them about any adjustments they may need to make to the operation of their unit based on measured conditions. Although it would be mainly limited to providing solar intensity and orientation of real-time measurements, it could be a cheap and effective feedback loop for the users of the unit to ensure operation is near optimal efficiency as much as possible and respond to any extreme events. Even in the most rural areas, this should be fairly feasible given the integration of the TE modules and battery for electricity provision. The application could include a filter for the feedstock composition and targeted byproducts to give detailed operational parameters based on specific implementation.

5. Conclusions

The design and feasibility assessment performed as part of this paper have provided an important step toward the deployment of solar pyrolysis unit for application in rural communities in SSA. The design process employed seems to have yielded an overall efficient system, particularly considering the cost minimization approach implemented, which should be able to achieve the pyrolysis of a broad range of biomass residues while enhancing sustainable development. SPEAR is also extremely simple to operate with minimal moving parts and labor requirements, which is likely to increase acceptance by local populations. A significant number of uncertainties remain, however, on how the system will perform in the field, which are essential to address in future work. The most important consideration in addressing these uncertainties regarding the overall feasibility of the system is the actual yield, composition and resulting soil amendment value of biochar as it is a major determinant in the added benefits produced by the unit. There is an abundance of studies on this topic, however, and thus, while no experimental data are available about our specific unit, reasonable assumptions aligned with the literature were made for feasibility assessment purposes. The actual optical efficiency of the CSP system at different locations and different times of year also ought to be investigated further in the future as the values presented for the representative site were merely intended as a proof-of-concept. The timeline and extent of the development of a carbon credit program in the region, whether through a communal or household-based system, is also going to be a major determinant in system uptake. The willingness of the local communities to divert agricultural waste streams from their current uses, however, must be investigated in more

detail as they currently associate crop productivity increases with these practices and are unfamiliar with the pyrolysis process. Nonetheless, if appropriate incentive mechanisms can be developed and the relevant uncertainties evaluated in more detail, SPEAR seems to present a reasonably feasible solution to synergistically address energy access and waste management issues within the urgency and timeframe required by their nature.

Author Contributions: Conceptualization of design C.C., O.M.; Methodology, O.M., C.C.; Modelling and feasibility assessment C.C.; Writing original draft C.C.; Review and editing O.M., C.C.; Supervision O.M. All authors have read and agreed to the published version of the manuscript.

Funding: This research received no external funding.

Institutional Review Board Statement: Not applicable.

Informed Consent Statement: Not applicable.

Data Availability Statement: The data presented in this study are available on request from the corresponding author.

Acknowledgments: The authors declare that no funding sources were involved in this work.

Conflicts of Interest: The authors declare no conflict of interest.

Appendix A. Unit Cost Breakdown for the System

Table A1. Unit cost breakdown.

Component	Cost Per Unit	Number Needed	Reference
Battery 220 Wh	95	1	[90]
TE 5.7 W	19.94/unit	5	[99]
DC connection cable (d = 4 mm, L = 95 mm)	0.49$/unit	10	[107]
Cement for insulation	7.4$ for a 50 kg bag	1	[108]
55-gallon (220 L) drum	10$ for new unit	1	[109]
Glass Steel PU sandwich mirror panel	39.1$/m^2	9.62 m^2	[110]
Faceted secondary reflector	49.7$/m^2	0.4016 m^2	[110]
30 cm diameter quartz window	29.95$	1	[111]
SiC Coated ceramic emitter plate	25.8$/plate	2	[112]
Char collection Drainage PVC pipe (d = 100 mm, L = 3 m)	9.36$	1	[113]
HRS 1573 K resistant silicon mix	7.99$ for 315 mL		[114]
843 K resistant Aluminum gasket for reactor top 550 mm	42.25$		[115]
Gasket clips and installation tools	15.4$		[115]
Perforated steel piping for gas collection (D = 32 mm, L = 500 mm)	7.5$	1	[116]
High skilled labor cost for 1 day	46.9$	1	[117]
FLOX™ Unit	56.68$/kWth	1.696 kWth	[118]
Stainless steel Ball Valve	2.2$/unit	1	[119]
Loop heat pipe	0.2$/W	575	[120]
Capillary heat pipe	0.1245$/W	750	[121]
5 W LEDs	1.99$/light	2	[69]
Dowtherm A HTF	4$/liter	1	[122]

Table A1. *Cont.*

Component	Cost Per Unit	Number Needed	Reference
Secondary reflector support telescopic poles (D = 6 mm, L = 1 m)	4.93$/piece	2	[123]
Primary concentrator aluminum telescopic poles (D = 25 mm, L = 1 m)	6.07$/piece	2	[123]
Telescopic tube connectors	3.12$/piece	4	[124]
Primary concentrator thermoplastic wheels (100 mm diameter)	3.64$/wheel	2	[125]

References

1. Gasser, T.; Luderer, G. Mitigation Pathways Compatible with 1.5 C in the Context of Sustainable Development. 2018. Available online: https://www.ipcc.ch/site/assets/uploads/sites/2/2019/05/SR15_Chapter2_Low_Res.pdf (accessed on 10 July 2019).
2. IEA. WEO-2017 Special Report: Energy Access Outlook. 2017. Available online: www.iea.org/t&c/ (accessed on 30 July 2019).
3. Hirmer, S.; Cruickshank, H. The user-value of rural electrification: An analysis and adoption of existing models and theories. *Renew. Sustain. Energy Rev.* **2014**, *34*, 145–154. [CrossRef]
4. Mertz, O.; Halsnæs, K.; Olesen, J.E.; Rasmussen, K. Adaptation to Climate Change in Developing Countries. *Environ. Manag.* **2009**, *43*, 743–752. [CrossRef]
5. PwC. Electricity beyond the Grid: Accelerating Access to Sustainable Power for All. 2016. Available online: www.pwc.com/utilities (accessed on 13 August 2019).
6. Lynd, L.R.; Sow, M.; Chimphango, A.F.; Cortez, L.A.; Brito Cruz, C.H.; Elmissiry, M.; Laser, M.; Mayaki, I.A.; Moraes, M.A.; Nogueira, L.A.; et al. Bioenergy and African transformation. *Biotechnol. Biofuels* **2015**, *8*, 18. [CrossRef]
7. Tucho, G.; Nonhebel, S.; Tucho, G.T.; Nonhebel, S. Bio-Wastes as an Alternative Household Cooking Energy Source in Ethiopia. *Energies* **2015**, *8*, 9565–9583. [CrossRef]
8. Das, K.C.; Singh, K.; Bibens, B.R.; Hilten, S.A.; Baker, W.D.; Greene, J.D. Peterson Pyrolysis Characteristics of Forest Residues Obtained from Different Harvesting Methods. *Appl. Eng. Agric.* **2013**, *27*, 107–113. [CrossRef]
9. World Bank. What a Waste 2.0: A Global Snapshot of Solid Waste Management to 2050. 2018, pp. 2–6. Available online: https://openknowledge.worldbank.org/handle/10986/30317 (accessed on 9 August 2019).
10. IEA. Biofuel Potential in Sub-Saharan Africa: Raising Food Yields, Reducing Food Waste and Utilising Residues. 2017. Available online: www.irena.org (accessed on 3 August 2019).
11. Lee, S.Y.; Sankaran, R.; Chew, K.W.; Tan, C.H.; Krishnamoorthy, R.; Chu, D.-T.; Show, P.-L. Waste to bioenergy: A review on the recent conversion technologies. *BMC Energy* **2019**, *1*, 4. [CrossRef]
12. Sharma, A.; Pareek, V.; Zhang, D. Biomass pyrolysis—A review of modelling, process parameters and catalytic studies. *Renew. Sustain. Energy Rev.* **2015**, *50*, 1081–1096. [CrossRef]
13. Kan, T.; Strezov, V.; Evans, T.J. Lignocellulosic biomass pyrolysis: A review of product properties and effects of pyrolysis parameters. *Renew. Sustain. Energy Rev.* **2016**, *57*, 1126–1140. [CrossRef]
14. Rony, A.H.; Kong, L.; Lu, W.; Dejam, M.; Adidharma, H.; Gasem, K.A.M.; Zheng, Y.; Norton, U.; Fan, M. Kinetics, thermodynamics, and physical characterization of corn stover (*Zea mays*) for solar biomass pyrolysis potential analysis. *Bioresour. Technol.* **2019**, *284*, 466–473. [CrossRef]
15. Antal, M.J.; Várhegyi, G.; Jakab, E. Cellulose Pyrolysis Kinetics: Revisited. *Ind. Eng. Chem. Res.* **1998**, *37*, 1267–1275. [CrossRef]
16. Gao, X.; Lu, L.; Shahnam, M.; Rogers, W.A.; Smith, K.; Gaston, K.; Robichaud, D.; Brennan Pecha, M.; Crowley, M.; Ciesielski, P.N.; et al. Assessment of a detailed biomass pyrolysis kinetic scheme in multiscale simulations of a single-particle pyrolyzer and a pilot-scale entrained flow pyrolyzer. *Chem. Eng. J.* **2021**, *418*, 129347. [CrossRef]
17. Yang, S.; Wang, S.; Wang, H. Particle-scale evaluation of the pyrolysis process of biomass material in a reactive gas-solid spouted reactor. *Chem. Eng. J.* **2020**, *21*, 127787. [CrossRef]
18. Lu, L.; Gao, X.; Gel, A.; Wiggins, G.M.; Crowley, M.; Pecha, B.; Shahnam, M.; Rogers, W.A.; Parks, J.; Ciesielski, P.N. Investigating biomass composition and size effects on fast pyrolysis using global sensitivity analysis and CFD simulations. *Chem. Eng. J.* **2020**, *21*, 127789. [CrossRef]
19. Mohan, D.; Abhishek, K.; Sarswat, A.; Patel, M.; Singh, P.; Pittman, C.U. Biochar production and applications in soil fertility and carbon sequestration–a sustainable solution to crop-residue burning in India. *RSC Adv.* **2018**, *8*, 508–520. Available online: http://xlink.rsc.org/?DOI=C7RA10353K9 (accessed on 10 August 2019). [CrossRef]
20. Galinato, S.P.; Yoder, J.K.; Granatstein, D. The economic value of biochar in crop production and carbon sequestration. *Energy Policy* **2011**, *39*, 6344–6350. Available online: https://www.sciencedirect.com/science/article/pii/S0301421511005672 (accessed on 10 August 2019). [CrossRef]
21. Archontoulis, S.V.; Huber, I.; Miguez, F.E.; Thorburn, P.J.; Rogovska, N.; Laird, D.A. A model for mechanistic and system assessments of biochar effects on soils and crops and trade-offs. *GCB Bioenergy* **2016**, *8*, 1028–1045. [CrossRef]

22. Park, J.; Lee, Y.; Ryu, C.; Park, Y.K. Slow pyrolysis of rice straw: Analysis of products properties, carbon and energy yields. *Bioresour. Technol.* **2014**, *155*, 63–70. [CrossRef]
23. Woolf, D.; Lehmann, J.; Lee, D.R. Optimal bioenergy power generation for climate change mitigation with or without carbon sequestration. *Nat. Commun.* **2016**, *7*, 13160. [CrossRef]
24. Roberts, K.G.; Gloy, B.A.; Joseph, S.; Scott, N.R.; Lehmann, J. Life cycle assessment of biochar systems: Estimating the energetic, economic, and climate change potential. *Environ. Sci. Technol.* **2010**, *44*, 827–833. [CrossRef] [PubMed]
25. Brown, T.R.; Wright, M.M.; Brown, R.C. Estimating profitability of two biochar production scenarios: Slow pyrolysis vs. fast pyrolysis. *Biofuels Bioprod. Biorefining* **2011**, *5*, 54–68. 4. [CrossRef]
26. Crombie, K.; Mašek, O. Investigating the potential for a self-sustaining slow pyrolysis system under varying operating conditions. *Bioresour. Technol.* **2014**, *162*, 148–156. [CrossRef]
27. Pereira, E.G.; Marchtins, M.A.; Pecenka, R.; Angélica de Cássia, O.C. Pyrolysis gases burners: Sustainability for integrated production of charcoal, heat and electricity. *Renew. Sustain. Energy Rev.* **2017**, *75*, 592–600. [CrossRef]
28. Wünning, J.A.; Wünning, J.G. Flameless oxidation to reduce thermal no-formation. *Prog. Energy Combust. Sci.* **1997**, *23*, 81–94. [CrossRef]
29. Blurock, E.; Battin-Leclerc, F. Modeling combustion with detailed kinetic mechanisms. In *Green Energy and Technology*; Springer: London, UK, 2013; pp. 17–57. Available online: https://www.springer.com/gp/book/9781447153061 (accessed on 15 July 2019). [CrossRef]
30. Yadav, D.; Banerjee, R. A review of solar thermochemical processes. *Renew. Sustain. Energy Rev.* **2016**, *54*, 497–532. [CrossRef]
31. Wieckert, C.; Obrist, A.; Von Zedtwitz, P.; Maag, G.; Steinfeld, A. Syngas Production by Thermochemical Gasification of Carbonaceous Waste Materials in a 150 kW th Packed-Bed Solar Reactor. *Energy Fuels* **2013**, *27*, 4770–4776. [CrossRef]
32. Morales, S.; Miranda, R.; Bustos, D.; Cazares, T.; Tran, H. Solar biomass pyrolysis for the production of bio-fuels and chemical commodities. *J. Anal. Appl. Pyrolysis* **2014**, *109*, 65–78. [CrossRef]
33. Garcia-Nunez, J.A.; Pelaez-Samaniego, M.R.; Garcia-Perez, M.E.; Fonts, I.; Abrego, J.; M Westerhof, R.J.; Garcia-Perez, M. Historical Developments of Pyrolysis Reactors: A Review. *Energy Fuels* **2017**, *31*, 5751–5775. Available online: https://pubs.acs.org/sharingguidelines (accessed on 17 July 2019). [CrossRef]
34. Chen, Q.; Yang, R.; Zhao, B.; Li, Y.; Wang, S.; Wu, H.; Zhuo, Y.; Chen, C. Investigation of heat of biomass pyrolysis and secondary reactions by simultaneous thermogravimetry and differential scanning calorimetry. *Fuel* **2014**, *134*, 467–476. [CrossRef]
35. Jahirul, M.I.; Rasul, M.G.; Chowdhury, A.A.; Ashwath, N. Biofuels production through biomass pyrolysis—A technological review. *Energies* **2012**, *5*, 4952–5001. [CrossRef]
36. Zeng, K.; Gauthier, D.; Soria, J.; Mazza, G.; Flamant, G. Solar pyrolysis of carbonaceous feedstocks: A review. *Sol. Energy* **2017**, *156*, 73–92. [CrossRef]
37. Adinberg, R.; Epstein, M.; Karni, J. Solar Gasification of Biomass: A Molten Salt Pyrolysis Study. *J. Sol. Energy Eng.* **2004**, *126*, 850. Available online: http://solarenergyengineering.asmedigitalcollection.asme.org/article.aspx?articleid=1457062 (accessed on 9 August 2019). [CrossRef]
38. Rony, A.H.; Mosiman, D.; Sun, Z.; Qin, D.; Zheng, Y.; Boman, J.H.; Fan, M. A novel solar powered biomass pyrolysis reactor for producing fuels and chemicals. *J. Anal. Appl. Pyrolysis* **2018**, *132*, 19–32. Available online: https://www-sciencedirect-com.ezproxy.is.ed.ac.uk/science/article/pii/S016523701830038X (accessed on 27 February 2019). [CrossRef]
39. Khairnasov, S.M.; Naumova, A.M. Heat pipes application to solar energy systems. *Appl. Sol. Energy (Engl. Transl. Geliotekhnika)* **2016**, *52*, 47–60. Available online: https://link.springer.com/article/10.3103/S0003701X16010060 (accessed on 29 January 2021). [CrossRef]
40. Steinfeld, A. Solar thermochemical production of hydrogen. In *Handbook of Hydrogen Energy*; CRC Press: Boca Raton, FL, USA, 2014.
41. Joardder, M.U.H.; Halder, P.K.; Rahim, M.A.; Masud, M.H. Solar Pyrolysis: Converting Waste Into Asset Using Solar Energy. *Clean Energy Sustain. Dev.* **2017**, 213–235.
42. Kodama, T. High-temperature solar chemistry for converting solar heat to chemical fuels. *Prog. Energy Combust. Sci.* **2003**, *29*, 567–597. Available online: https://www.sciencedirect.com/science/article/pii/S0360128503000595 (accessed on 11 July 2019). [CrossRef]
43. Zeaiter, J.; Ahmad, M.N.; Rooney, D.; Samneh, B.; Shammas, E. Design of an automated solar concentrator for the pyrolysis of scrap rubber. *Energy Convers. Manag.* **2015**, *101*, 118–125. [CrossRef]
44. Chintala, V.; KuMarch, S.; Pandey, J.K.; Sharma, A.K.; KuMarch, S. Solar thermal pyrolysis of non-edible seeds to biofuels and their feasibility assessment. *Energy Convers. Manag.* **2017**, *153*, 482–492. [CrossRef]
45. Li, R.; Zeng, K.; Soria, J.E.; Gauthier, D.; Rodriguez, R.; Flamant, G. Product distribution from solar pyrolysis of agricultural and forestry biomass residues. *Renew. Energy* **2015**, *89*, 27–35. Available online: doi.org/10.1016/j.renene.2015.11.071 (accessed on 9 August 2019).
46. Zeng, K.; Gauthier, D.; Li, R.; Flamant, G. Solar pyrolysis of beech wood: Effects of pyrolysis parameters on the product distribution and gas product composition. *Energy* **2015**, *93*, 1648–1657. [CrossRef]
47. Daugaard, D.E.; Brown, R.C. Enthalpy for Pyrolysis for Several Types of Biomass Enthalpy for Pyrolysis for Several Types of Biomass Enthalpy for Pyrolysis for Several Types of Biomass. *Energy Fuels* **2003**, *17*, 934–939. [CrossRef]
48. World Bank. Global Wind Atlas. 2019. Available online: https://globalwindatlas.info/ (accessed on 1 August 2019).

49. World Bank. Global Solar Atlas. 2019. Available online: https://globalsolaratlas.info/ (accessed on 30 July 2019).
50. World Bank. Inflation, consumer prices (annual %)-Sub-Saharan Africa, Middle East & North Africa. 2021. Available online: https://data.worldbank.org/indicator/FP.CPI.TOTL.ZG?locations=ZG-ZQ (accessed on 10 August 2019).
51. Titiloye, J.O.; Abu Bakar, M.S.; Odetoye, T.E. Thermochemical characterisation of agricultural wastes from West Africa. *Ind. Crops Prod.* **2013**, *47*, 199–203. [CrossRef]
52. Ackerman, P.; Ham, C.; Dovey, S.; Du Toit, B.; De Wet, J.; Kunneke, A.; Seifert, T.; Meincken, M.; Von Doderer, C. The Use of Forest Residue for Bioenergy in Southern Africa. 2013. Available online: https://www.icfr.ukzn.ac.za/sites/default/files/pubs/Bulletin03-2013.pdf (accessed on 4 August 2019).
53. Dasappa, S. Potential of biomass energy for electricity generation in sub-Saharan Africa. *Energy Sustain. Dev.* **2014**, *15*, 203–213. Available online: https://www.sciencedirect.com/science/article/pii/S0973082611000524 (accessed on 22 November 2018). [CrossRef]
54. Onsree, T.; Tippayawong, N.; Zheng, A.; Li, H. Pyrolysis behavior and kinetics of corn residue pellets and eucalyptus wood chips in a macro thermogravimetric analyzer. *Case Stud. Therm. Eng.* **2018**, *12*, 546–556. Available online: https://www.sciencedirect.com/science/article/pii/S2214157X18301424 (accessed on 4 August 2019). [CrossRef]
55. The Cary Company. Specs: 55 Gallon Blue Tight Head Plastic Drum, UN Rated, 2"NPS & 2" Buttress Fittings. 2019. Available online: https://www.thecarycompany.com/media/pdf/specs/56W55D.pdf (accessed on 3 August 2019).
56. Mohammad, S.T.; Al-Kayiem, H.H.; Assadi, M.K.; Kananda, K.; Nazir, R.; Jadhav, S. Thermal losses in central receiver solar thermal power plant Related content Performance and Simulation of a Stand-alone Parabolic Trough Solar Thermal Power Plant Numerical Investigation on Trapezoidal Cavity Receiver Used In LFR with Water Flow in Absor. 2018. Available online: https://iopscience.iop.org/article/10.1088/1757-899X/377/1/012008/pdf (accessed on 1 August 2019).
57. Steinfeld, A.; Schubnell, M. Optimum aperture size and operating temperature of a solar cavity-receiver. *Sol. Energy* **1993**, *50*, 19–25. [CrossRef]
58. Shuai, Y.; Xia, X.L.; Tan, H.P. Radiation performance of dish solar concentrator/cavity receiver systems. *Sol. Energy* **2008**, *82*, 13–21. [CrossRef]
59. Steinfeld, A.; Brack, M.; Meier, A.; Weidenkaff, A.; Wuillemin, D. A solar chemical reactor for co-production of zinc and synthesis gas. *Energy* **1998**, *23*, 803–814. [CrossRef]
60. Jouhara, H.; Nannou, T.K.; Anguilano, L.; Ghazal, H.; Spencer, N. Heat pipe based municipal waste treatment unit for home energy recovery. *Energy* **2017**, *139*, 1210–1230. [CrossRef]
61. Yang, H.; Kudo, S.; Kuo, H.-P.; Norinaga, K.; Mori, A.; Mašek, O.; Hayashi, J. Estimation of Enthalpy of Bio-Oil Vapor and Heat Required for Pyrolysis of Biomass. *Energy Fuels* **2013**, *27*, 2675–2686. Available online: http://pubs.acs.org/doi/10.1021/ef400199z (accessed on 28 July 2019). [CrossRef]
62. Kalogirou, S.A. Solar thermal collectors and applications. *Prog. Energy Combust. Sci.* **2004**, *30*, 231–295. [CrossRef]
63. Ferrer-Rodríguez, J.P.; Fernández, E.F.; Almonacid, F.; Pérez-Higueras, P. Geometric Optical Design; (350.6050) Solar Energy; (220.1770) Concentrators; (220.4298) Nonimaging Optics. 2016. Available online: http://dx.doi.org/10.1364/OL.41.001985 (accessed on 30 July 2019).
64. Shanks, K.; Sarmah, N.; Ferrer-Rodriguez, J.P.; Senthilarasu, S.; Reddy, K.S.; Fernández, E.F.; Mallick, T. Theoretical investigation considering manufacturing errors of a high concentrating photovoltaic of cassegrain design and its experimental validation. *Sol. Energy* **2016**, *131*, 235–245. Available online: https://www.sciencedirect.com/science/article/pii/S0038092X16001596#b0110 (accessed on 16 July 2019). [CrossRef]
65. TracePro TracePro Tutorials Archives | Lambdares.com. Available online: https://www.lambdares.com/su/tracepro-tutorials/ (accessed on 30 July 2019).
66. SunEarthTools Sun-Earth Tools: Calculation of Sun's Position in the Sky for Each Location on the Earth at Any Time of Day. Available online: https://www.sunearthtools.com/dp/tools/pos_sun.php (accessed on 1 August 2019).
67. Borchers, A.M.; Duke, J.M.; Parsons, G.R. Does willingness to pay for green energy differ by source? *Energy Policy* **2007**, *35*, 3327–3334. [CrossRef]
68. ESMAP. Measuring Energy Access Introduction to the Multi-Tier Framework. 2015. Available online: https://www.seforall.org/sites/default/files/MTFpresentation_SE4ALL_April5.PDF (accessed on 10 August 2019).
69. Amazon 25 Year Life Philips My Vision LED 5w Light Bulb BC B22 Bayonet Cap Warm White 2700k GLS Standard Shape Instant Low Energy Saving 250 Lumen Lamps L.E.D. [Energy Class A]. Available online: https://www.amazon.co.uk/Philips-Vision-Bayonet-Standard-Instant/dp/B0083WDMPW (accessed on 10 August 2019).
70. Toolbox, E. Fuels-Higher and Lower Calorific Values. Available online: https://www.engineeringtoolbox.com/fuels-higher-calorific-values-d_169.html (accessed on 10 August 2019).
71. WorldBank. Pump Price for Diesel Fuel (US$ per liter) | Data. Available online: https://data.worldbank.org/indicator/EP.PMP.DESL.CD (accessed on 10 August 2019).
72. Reber, T.; Booth, S.; Cutler, D.; Li, X.; Salasovich, J. Tariff Considerations for Micro-Grids in Sub-Saharan Africa. 2018. Available online: www.nrel.gov/publications (accessed on 10 August 2019).
73. Rosnes, O.; Vennemo, H. The cost of providing electricity to Africa. *Energy Econ.* **2012**, *34*, 1318–1328. [CrossRef]

74. IDS. The Costs and Benefits of Lighting and Electricity Services for Off-Grid Populations in Sub-Sahara Africa. 2018. Available online: https://assets.publishing.service.gov.uk/media/5af96657ed915d0df4e8cdea/Costs_Benefits_Off-Grid_Electricity_Lighting_Systems.pdf (accessed on 10 August 2019).
75. Megan, D. South Africa's Ramaphosa Signs Carbon Tax into Law. Available online: https://www.climatechangenews.com/2019/05/28/south-africas-ramaphosa-signs-carbon-tax-law/ (accessed on 15 July 2019).
76. Stig, S. The MSR: Impact on Marchket balance and prices. *Point Carbon Thomson Reuters* **2019**. Available online: https://ec.europa.eu/clima/sites/clima/files/docs/0094/thomson_reuters_point_carbon_en.pdf (accessed on 15 July 2019).
77. Mondal, M.A.H.; Bryan, E.; Ringler, C.; Rosegrant, M. Ethiopian power sector development: Renewable based universal electricity access and export strategies. *Renew. Sustain. Energy Rev.* **2017**, *75*, 11–20. Available online: https://www-sciencedirect-com.ezproxy.is.ed.ac.uk/science/article/pii/S1364032116306979 (accessed on 25 November 2018). [CrossRef]
78. Gwenzi, W.; Chaukura, N.; Mukome, F.N.D.; Machado, S.; Nyamasoka, B. Biochar production and applications in sub-Saharan Africa: Opportunities, constraints, risks and uncertainties. *J. Environ. Manag.* **2015**, *150*, 250–261. Available online: https://linkinghub.elsevier.com/retrieve/pii/S0301479714005684 (accessed on 13 June 2019). [CrossRef] [PubMed]
79. Weitzman, M.L. A Review of the Stern Review on the Economics of Climate Change. *J. Econ. Lit.* **2007**, *45*, 703–724. Available online: http://pubs.aeaweb.org/doi/10.1257/jel.45.3.703 (accessed on 11 August 2019). [CrossRef]
80. TEG. Thermoelectric Gencell Technology. Available online: www.Tecteg.com (accessed on 4 August 2019).
81. Stewart, M.; Stewart, M. Piping system components. *Surf. Prod. Oper.* **2016**, 193–300. Available online: https://www.sciencedirect.com/science/article/pii/B9781856178082000043 (accessed on 4 August 2019).
82. Ghosh, A.; Ghosh, A.; Neogi, S. Evaluation of physical and thermal properties of coal combustion residue blended concrete for energy efficient building application in India. *Adv. Build. Energy Res.* **2018**, 1–22. Available online: https://www.tandfonline.com/doi/full/10.1080/17512549.2018.1557076 (accessed on 1 August 2019).
83. Narendra Babu, N.; Kamath, H.C. Materials used in Heat Pipe. *Mater. Today Proc.* **2015**, *2*, 1469–1478. Available online: https://linkinghub.elsevier.com/retrieve/pii/S221478531500317X (accessed on 3 August 2019). [CrossRef]
84. Tang, Y.; Zhou, R.; Lu, L.; Xie, Z. Anti-Gravity Loop-shaped heat pipe with graded pore-size wick. *Appl. Therm. Eng.* **2012**, *36*, 78–86. Available online: https://www.sciencedirect.com/science/article/pii/S135943111100723X#bib14 (accessed on 19 July 2019). [CrossRef]
85. A Product Technical Data DOWTHERM A Heat Transfer Fluid. Available online: http://www.dow.com/heattrans (accessed on 3 August 2019).
86. Jouhara, H.; Chauhan, A.; Nannou, T.; Almahmoud, S.; Delpech, B.; Wrobel, L.C. Heat pipe based systems—Advances and applications. *Energy* **2017**, *128*, 729–754. Available online: https://www.sciencedirect.com/science/article/pii/S0360544217305935 (accessed on 22 July 2019). [CrossRef]
87. Pihl, E.; Kushnir, D.; Sandén, B.; Johnsson, F. Material Constraints for Concentrating Solar Thermal Power. *Energy* **2012**, *44*, 944–954. Available online: http://fossilhub.org/wp-content/uploads/2014/03/Pihl_etal2012_ConcSolarPower_materials.pdf (accessed on 12 August 2019).
88. Hijazi, H.; MokhiaMarch, O.; Elsamni, O. Mechanical design of a low cost parabolic solar dish concentrator. *Alex. Eng. J.* **2016**, *55*, 1–11. Available online: https://www.sciencedirect.com/science/article/pii/S111001681600034X (accessed on 14 July 2019). [CrossRef]
89. Lertsatitthanakorn, C.; Jamradloedluk, J.; Rungsiyopas, M. Electricity generation from a solar parabolic concentrator coupled to a thermoelectric module. *Energy Procedia* **2014**, *52*, 150–158. Available online: http://dx.doi.org/10.1016/j.egypro.2014.07.065 (accessed on 19 July 2019). [CrossRef]
90. Alibaba Portable Power Station 220wh Emergency Backup Lithium Battery 200w Ac Inverter Outlet Solar Generator-Buy Rechargable Batteries, Solar Power Bank, Camping Back Up Power Product on Alibaba.com. Available online: https://www.alibaba.com/product-detail/Portable-Power-Station-220Wh-Emergency-Backup_62055629175.html?spm=a2700.7724857.normalList.34.2747d8c4VueH1R (accessed on 12 August 2019).
91. Rueda-Ordóñez, Y.J.; Tannous, K.; Olivares-Gómez, E. An empirical model to obtain the kinetic parameters of lignocellulosic biomass pyrolysis in an independent parallel reactions scheme. *Fuel Process. Technol.* **2015**, *140*, 222–230. Available online: https://www.sciencedirect.com/science/article/pii/S0378382015301557 (accessed on 12 August 2019). [CrossRef]
92. Supin, S.; Buathong, C.; Sirisak, S. High-energy conversion efficiency of drum kiln with heat distribution pipe for charcoal and biochar production. *Energy Sustain. Dev.* **2019**, *59*, 1–7.
93. Jouhara, H.; Ahmad, D.; van den Boogaert, I.; Katsou, E.; Simons, S.; Spencer, N. Pyrolysis of domestic based feedstock at temperatures up to 300 °C. *Therm. Sci. Eng. Prog.* **2018**, *5*, 117–143. Available online: https://www.sciencedirect.com/science/article/pii/S2451904917303980#b0165 (accessed on 24 July 2019). [CrossRef]
94. Busch, J.; Lubowski, R.N.; Godoy, F.; Steininger, M.; Yusuf, A.A.; Austin, K.; Hewson, J.; Juhn, D.; Farid, M.; Boltz, F. Structuring economic incentives to reduce emissions from deforestation within Indonesia. *Proc. Natl. Acad. Sci. USA* **2012**, *109*, 1062–1067. Available online: http://www.ncbi.nlm.nih.gov/pubmed/22232665 (accessed on 29 November 2018). [CrossRef] [PubMed]
95. IRENA. Solar PV in Africa: Costs and Marchkets. 2016. Available online: www.irena.org (accessed on 29 January 2021).
96. Alston, S.M.; Arnold, J.C. Environmental Impact of Pyrolysis of Mixed WEEE Plastics Part 2: Life Cycle Assessment. *Environ. Sci. Technol.* **2011**, *45*, 9386–9392. Available online: https://pubs.acs.org/doi/10.1021/es2016654 (accessed on 13 August 2019). [CrossRef]

97. Mcelligott, K.M.; Coleman, M. Biochar Amendments to Forest Soils: Effects on Soil Properties and Tree Growth. 2011. Available online: https://forest.moscowfsl.wsu.edu/smp/solo/documents/GTs/McElligott-Kristin_Thesis.pdf (accessed on 14 August 2019).
98. Acumen. How Affordable is Off-Grid Energy Access in Africa? An Evidence Review. 2017. Available online: https://acumen.org/wp-content/uploads/2017/07/Evidence-Review-On-Affordability.pdf (accessed on 10 August 2019).
99. TEG. Recycling Waste Heat for a Cooler Tomorrow Recycling Waste Heat for a Cooler Tomorrow Product Overview Geometric Characteristics. 2015. Available online: www.tegpro.com (accessed on 4 August 2019).
100. Mitchell, E.J.S.; Ting, Y.; Allan, J.; Lea-Langton, A.R.; Spracklen, D.V.; McFiggans, G.; Coe, H.; Routledge, M.N.; Williams, A.; Jones, J.M. Pollutant Emissions from Improved Cookstoves of the Type Used in Sub-Saharan Africa. *Combust. Sci. Technol.* **2020**, *192*, 1582–1602. Available online: https://www.tandfonline.com/doi/full/10.1080/00102202.2019.1614922 (accessed on 17 February 2021). [CrossRef]
101. Kshirsagar, M.P.; Kalamkar, V.R. A comprehensive review on biomass cookstoves and a systematic approach for modern cookstove design. *Renew. Sustain. Energy Rev.* **2014**, *30*, 580–603. [CrossRef]
102. Champier, D.; Bédécarrats, J.P.; Kousksou, T.; Rivaletto, M.; Strub, F.; Pignolet, P. Study of a TE (thermoelectric) generator incorporated in a multifunction wood stove. *Energy* **2011**, *36*, 1518–1526. [CrossRef]
103. Torres-Rojas, D.; Lehmann, J.; Hobbs, P.; Joseph, S.; Neufeldt, H. Biomass availability, energy consumption and biochar production in rural households of Western Kenya. *Biomass Bioenergy* **2011**, *35*, 3537–3546. [CrossRef]
104. Tian, Y.; Zhao, C.Y. A review of solar collectors and thermal energy storage in solar thermal applications. *Appl. Energy* **2013**, *104*, 538–553. [CrossRef]
105. Renewable Energy Agency I. Renewable Energy Technologies: Cost Analysis Series Concentrating Solar Power Volume 1: Power Sector Issue 2/5 Acknowledgement. 2012. Available online: www.irena.org/Publications (accessed on 14 July 2019).
106. Schöniger, F.; Thonig, R.; Resch, G.; Lilliestam, J. Making the sun shine at night: Comparing the cost of dispatchable concentrating solar power and photovoltaics with storage. *Energy Sources Part B Econ. Plan. Policy* **2021**, 1–20. Available online: https://www.tandfonline.com/doi/full/10.1080/15567249.2020.1843565 (accessed on 17 February 2021).
107. 4 mm Black PV Solar Cable. Available online: https://quickbit.co.uk/4mm-solar-cable?language=en&currency=GBP&gclid=CjwKCAjw1rnqBRAAEiwAr29II8-PhcQYS49G8X_dpH6XJDvedi9kJkYY15CVQPUMHydetsfP9i9khRoCbo0QAvD_BwE (accessed on 10 August 2019).
108. Cement: Constructing Africa—CAHF | Centre for Affordable Housing Finance Africa. Available online: http://housingfinanceafrica.org/cement-constructing-africa/ (accessed on 10 August 2019).
109. Gallon Steel Drums For Sale—Buy 55 Gallon Steel Drums For Sale, 55 Gallon Steel Drums For Sale, 55 Gallon Steel Drums For Sale Product on Alibaba.com. Available online: https://www.alibaba.com/product-detail/55-gallon-steel-drums-for-sale_62022559768.html?spm=a2700.7724857.main07.10.53947624kGFb9A (accessed on 10 August 2019).
110. Dish systems for CSP. Available online: https://www.osti.gov/pages/servlets/purl/1356835 (accessed on 10 August 2019).
111. Quartz Windows | Fluorescence Applications | UV Fused Silica. Available online: https://www.knightoptical.com/stock/optical-components/uvvisnir-optics/windows/quartz-uv-fused-silica-ir-quartz-windows/quartz-windows/ (accessed on 10 August 2019).
112. Silicon Carbide Plates High Temperature and Corrosion Resistance Ceramic Plate Boards—Buy Silicon Carbide Plates, Ceramic Plate, Ceramic Plate Boards Product on Alibaba.com. Available online: https://www.alibaba.com/product-detail/Silicon-Carbide-Plates-High-Temperature-And_62022936406.html?spm=a2700.7724857.normalList.11.3fde6ecdRWXDCO&s=p (accessed on 10 August 2019).
113. Drainage Pipe Plain Ended—110mm x 3mtr. Available online: https://www.drainagepipe.co.uk/drainage-pipe-plain-ended-110mm-x-3mtr-p-D043/ (accessed on 10 August 2019).
114. Heat Resistant Sealant 310 mL in Cartridge Gun Tube | VITCAS. Available online: https://shop.vitcas.com/vitcas-heat-resistant-sealant-1300.html (accessed on 10 August 2019).
115. Kurt, J. Lesker Company | Aluminum Gaskets for CF Flanges | Vacuum Science Is Our Business. Available online: https://www.lesker.com/newweb/flanges/hardware_cf_gaskets.cfm?pgid=aluminum (accessed on 10 August 2019).
116. Perforated Pipes Exhaust Tube T304 Stainless Steel All Sizes Pipe Length Tubes | eBay. Available online: https://www.ebay.co.uk/itm/Perforated-Pipes-Exhaust-Tube-T304-Stainless-Steel-All-Sizes-Pipe-Length-Tubes-/233013535235 (accessed on 10 August 2019).
117. 3.4 Malawi Manual Labor Costs—Logistics Capacity Assessment—Digital Logistics Capacity Assessments. Available online: https://dlca.logcluster.org/display/public/DLCA/3.4+Malawi+Manual+Labor+Costs (accessed on 10 August 2019).
118. A techno-economic analysis of the application of continuous staged-combustion and flameless oxidation to the combustor design in gas turbines. *Fuel Process. Technol.* **2006**, *87*, 727–736. Available online: https://www-sciencedirect-com.ezproxy.is.ed.ac.uk/science/article/pii/S037838200600035X (accessed on 10 August 2019). [CrossRef]
119. Stainless Steel Cf8 100 mm 1000 Wog Bspt Screw End Ball Valve With Limit Switch—Buy Ball Valve with Limit Switch, Bspt Screw End Ball Valve, Bspt Screw End Ball Valve With Limit Switch Product on Alibaba.com. Available online: https://www.alibaba.com/product-detail/Stainless-steel-cf8-100mm-1000-wog_60690079515.html?spm=a2700.7724857.normalList.38.56d52ef0M6ylmO (accessed on 10 August 2019).
120. Huang, B.J.; Chuang, Y.H.; Yang, P.E. Low-cost manufacturing of loop heat pipe for commercial applications. *Appl. Therm. Eng.* **2017**, *126*, 1091–1097. Available online: http://dx.doi.org/10.1016/j.applthermaleng.2016.12.062 (accessed on 9 August 2019). [CrossRef]

121. CCI Copper Heat Pipe and Sink Specifications. Available online: http://www.farnell.com/datasheets/317989.pdf?_ga=2.156455410.857736183.1565447970-136742991.1565447970&_gac=1.79837925.1565447970.CjwKCAjw1rnqBRAAEiwAr29II_DFeKwUcwYinKkQXa-stZJvD2RXvSLAbOV__o8QKxXfoFZMmP0shxoCJvoQAvD_BwE (accessed on 10 August 2019).
122. Dowtherm A—Buy Dowtherm A Biphenyl Diphenyl Oxide Eutectic, Dowtherm A Oem Diphenyl And Diphenylether, Dowtherm A Oem Heat Transfer Fluid Polyester Production Use Product on Alibaba.com. Available online: https://www.alibaba.com/product-detail/Equal-to-Dowtherm-A_60599873147.html?spm=a2700.7724857.normalList.1.61741db1zvofVc (accessed on 12 August 2019).
123. 1/2in OD Telescopic Tube | Aluminium | metals4U. Available online: https://www.metals4u.co.uk/aluminium/c1/telescopic-tube/c177/12.7mm-(-12-)-od/p3051 (accessed on 14 August 2019).
124. 1in to 7/8in Adjustable Tube Connector | Aluminium | metals4U. Available online: https://www.metals4u.co.uk/aluminium/c1/telescopic-tube/c177/1-to-78-adjustable-connector/p3061 (accessed on 14 August 2019).
125. 100 mm Grey non Marchking Thermoplastic Rubber Wheel. Available online: https://www.rosscastors.co.uk/100mm-grey-non-Marchking-thermoplastic-rubber-wheel.html?utm_source=google_shopping&gclid=Cj0KCQjw4s7qBRCzARIsAImcAxZuJB3hdSxwRfav_ukKFYkbf0BhauKTv5My7ME8m-3jgA6ltU8IMWUaAvW3EALw_wcB (accessed on 14 August 2019).